

4. LATE QUATERNARY STRATIGRAPHY AND SEDIMENTATION AT SITE 1002, CARIACO BASIN (VENEZUELA)¹

L.C. Peterson,² G.H. Haug,³ R.W. Murray,⁴ K.M. Yarincik,⁴ J.W. King,⁵ T.J. Bralower,⁶
K. Kameo,⁷ S.D. Rutherford,⁵ and R.B. Pearce⁸

ABSTRACT

Ocean Drilling Program Site 1002 in the Cariaco Basin was drilled in the final two days of Leg 165 with only a short transit remaining to the final port of San Juan, Puerto Rico. Because of severe time constraints, cores from only the first of the three long replicate holes (Hole 1002C) were opened at sea for visual description, and the shipboard sampling was restricted to the biostratigraphic examination of core catchers. The limited sampling and general scarcity of biostratigraphic datums within the late Quaternary interval covered by this greatly expanded hemipelagic sequence resulted in a very poorly defined age model for Site 1002 as reported in the Leg 165 *Initial Reports* volume of the *Proceedings of the Ocean Drilling Program*. Here, we present for the first time a new integrated stratigraphy for Site 1002 based on the standard of late Quaternary oxygen-isotope variations linked to a suite of refined biostratigraphic datums. These new data show that the sediment sequence recovered by Leg 165 in the Cariaco Basin is continuous and spans the time interval from 0 to ~580 ka, with a basal age roughly twice as old as initially suspected from the tentative shipboard identification of a single biostratigraphic datum. Lithologic subunits recognized at Site 1002 are here tied into this new stratigraphic framework, and temporal variations in major sediment components are reported. The biogenic carbonate, opal, and organic carbon contents of sediments in the Cariaco Basin tend to be high during interglacials, whereas the terrigenous contents of the sediments increase during glacials. Glacioeustatic variations in sea level are likely to exert a dominant control on these first-order variations in lithology, with glacial surface productivity and the nutrient content of waters in the Cariaco Basin affected by shoaling glacial sill depths, and glacial terrigenous inputs affected by narrowing of the inner shelf and increased proximity of direct riverine sources during sea-level lowstands.

INTRODUCTION

Ocean Drilling Program (ODP) Site 1002 is located in the Cariaco Basin, a structural depression on the northern continental shelf of Venezuela which, after the Black Sea, is the largest anoxic marine basin in the world. Since recovery of the first sediment cores from this basin in the late 1950s, it has been known that laminated deposits that accumulate in its depths are nearly undisturbed by bioturbation and contain well-preserved assemblages of both calcareous and siliceous microfossils (Heezen et al., 1958, 1959). High sedimentation rates (300 to >1000 m/m.y.) and location in a climatically sensitive region of the tropical ocean made the Cariaco Basin a prime drilling target on Leg 165 for high-resolution studies of geologically recent climate change.

The major objectives at Site 1002 were to recover a continuous and undisturbed upper Quaternary stratigraphic section that could be used to (1) document how climate change in the southern Caribbean and northern South America relates to climatic forcing mechanisms and to global-scale change, especially to high-latitude changes recorded in ice cores and in other high-deposition-rate marine sediment

sequences; (2) study the rates and magnitudes of tropical climate change at interannual to millennial time scales over the last several glacial-interglacial cycles; (3) examine the stability of tropical climate in response to past changes in large-scale global boundary conditions; and (4) study the relationships between climate variability and processes that influence the burial of organic carbon in anoxic settings. The recovery objectives were successfully achieved with the drilling of five holes at Site 1002, two of which were single mudline cores taken for geochemical studies, and three that were taken for high-resolution paleoclimatic reconstructions and that together penetrated to a maximum depth of 170.1 meters below seafloor (mbsf).

Site 1002 came at the very end of Leg 165, with only 2 days allocated for drilling, followed by a short transit (~1.5 days) to the final port of San Juan, Puerto Rico. Given the advance realization that normal shipboard processing of Site 1002 cores would be impossible in the available time, special provisions were made whereby only cores from the first of the long holes, Hole 1002C, were opened on board ship for initial description and preliminary sampling. The limited time for sampling and the general scarcity of biostratigraphic datums within the hemipelagic sediments of late Quaternary age resulted in a very poorly defined age model for Site 1002 as reported in the Leg 165 *Initial Reports* volume of the *Proceedings of the Ocean Drilling Program* (Sigurdsson, Leckie, Acton, et al., 1997). The tentative shipboard identification of *Emiliana huxleyi* at the base of the sequence initially indicated that all of the sediments recovered at Site 1002 lie within calcareous nannofossil Zone CN15 of Okada and Bukry (1980), suggesting a basal age of the site of no more than 248 ka. Our shore-based studies have subsequently shown this estimate to be in error and have led to a new integrated stratigraphy based on the standard of late Quaternary oxygen-isotope variations linked to a refined biostratigraphic framework. The purpose of this paper is to formally present the revised stratigraphy for this site and to tie in and discuss temporal changes in the sediment lithologies in the context of late Quaternary climate cycles.

¹Leckie, R.M., Sigurdsson, H., Acton, G.D., and Draper, G. (Eds.), 2000. *Proc ODP, Sci. Results*, 165: College Station, TX (Ocean Drilling Program).

²Rosenstiel School of Marine and Atmospheric Science, University of Miami, Miami, FL 33149, U.S.A. lpeterson@rsmas.miami.edu

³Department of Earth Sciences, University of Southern California, Los Angeles, CA 90089, U.S.A.

⁴Department of Earth Sciences, Boston University, Boston, MA 02215, U.S.A.

⁵Graduate School of Oceanography, University of Rhode Island, Narragansett, RI 02882, U.S.A.

⁶Department of Geology, University of North Carolina, Chapel Hill, NC 27599, U.S.A.

⁷Teikoku Oil Co., Ltd., 1-31-10, Hatagaya, Shibuya 151-856, Tokyo, Japan.

⁸School of Ocean and Earth Science, University of Southampton, Southampton Oceanography Centre, Southampton SO14 3ZH, United Kingdom.

BACKGROUND

Regional Setting and Hydrography

The Cariaco Basin (Fig. 1) is a small, east-west-trending pull-apart basin (Schubert, 1982) located on the northern continental shelf of eastern Venezuela. What is called the Cariaco Basin (or Trench) actually consists of two small sub-basins, each reaching depths of ~1400 m, separated by a central saddle that shoals to ~900 m. Along its northern margin, the Cariaco Basin is separated from the open Caribbean by the shallow Tortuga Bank that extends from Margarita Island west to Cabo Codera on the Venezuelan mainland. The surrounding topography and the shallow inlet sills (<146 m) together limit the exchange of deep waters with the rest of the Caribbean. This, combined with the excessive oxygen demand created by high upwelling-induced surface productivity, results in the present anoxic conditions below a water depth of ~300 m (see Richards [1975] and Peterson et al. [1991] for more detailed discussions of the local hydrography). The almost complete lack of bioturbation imposed by the absence of oxygen leads to preservation of a nearly undisturbed recent sediment record.

Upwelling of cold, nutrient-rich waters occurs seasonally along the northern Venezuelan coast in response to changes in the prevailing trade-wind field driven by the annual movement of the Intertropical Convergence Zone (ITCZ) (e.g., Wüst, 1964; Hastenrath, 1978; Muller-Karger and Aparicio-Castro, 1994). Between January and March, when the ITCZ is south of the equator, strong trade winds in the tropical North Atlantic induce a slow Ekman drift to the west and northwest. This drift helps maintain the North Brazil and Guyana Current systems that direct flow northwestward toward the Caribbean as part of the surface limb of the Atlantic's "conveyor belt" circulation (e.g., Broecker, 1992). At the same time, the trade winds blowing along the northern coast of Venezuela result in intense Ek-

man drift-induced upwelling of cool, nutrient-rich waters. In the Cariaco Basin, vertical advection is generally most active during January and February, with isotherms raised by as much as 175 m and sea-surface temperatures (SSTs) recorded as cool as 22°C (Herrera and Febres-Ortega, 1975). Regionally, the upwelling season is also the dry season because the ITCZ, along with its associated low pressure and rainfall, lies at its southernmost position.

Beginning in about June or July, as the ITCZ moves north to a position near the Venezuelan coast (6° – 10° N), the trade winds diminish and the coastal upwelling weakens or is largely shut off. Sea-surface temperatures over the Cariaco Basin typically warm to 27° – 28° C. Northward motion of the ITCZ triggers the rainy season north of $\sim 5^{\circ}$ N (Hastenrath, 1990), which has a strong influence on sea-surface salinity in the western tropical Atlantic and southern Caribbean through the discharge of the Amazon and Orinoco Rivers, as well as the smaller local rivers that drain directly into the Cariaco Basin (Dessier and Donguy, 1994). Sediments of the Cariaco Basin thus offer the important opportunity to reconstruct late Quaternary variability in the circulation of the tropical atmosphere and ocean, and to examine changes in the regional hydrologic balance over northern South America.

Cariaco Basin Sediments

Heezen et al. (1958, 1959) were the first to report the characteristics of Cariaco Basin sediments based on twelve piston cores collected during a *Vema* cruise in 1957. Athearn (1965) later described a suite of more than 20 cores collected by the Woods Hole Oceanographic Institution in the early 1960s, whereas Lidz et al. (1969) contributed additional descriptions based on cores collected by the University of Miami in 1966. In 1970, Deep Sea Drilling Project (DSDP) Site 147 was drilled by the *Glomar Challenger* on the western edge of the cen-

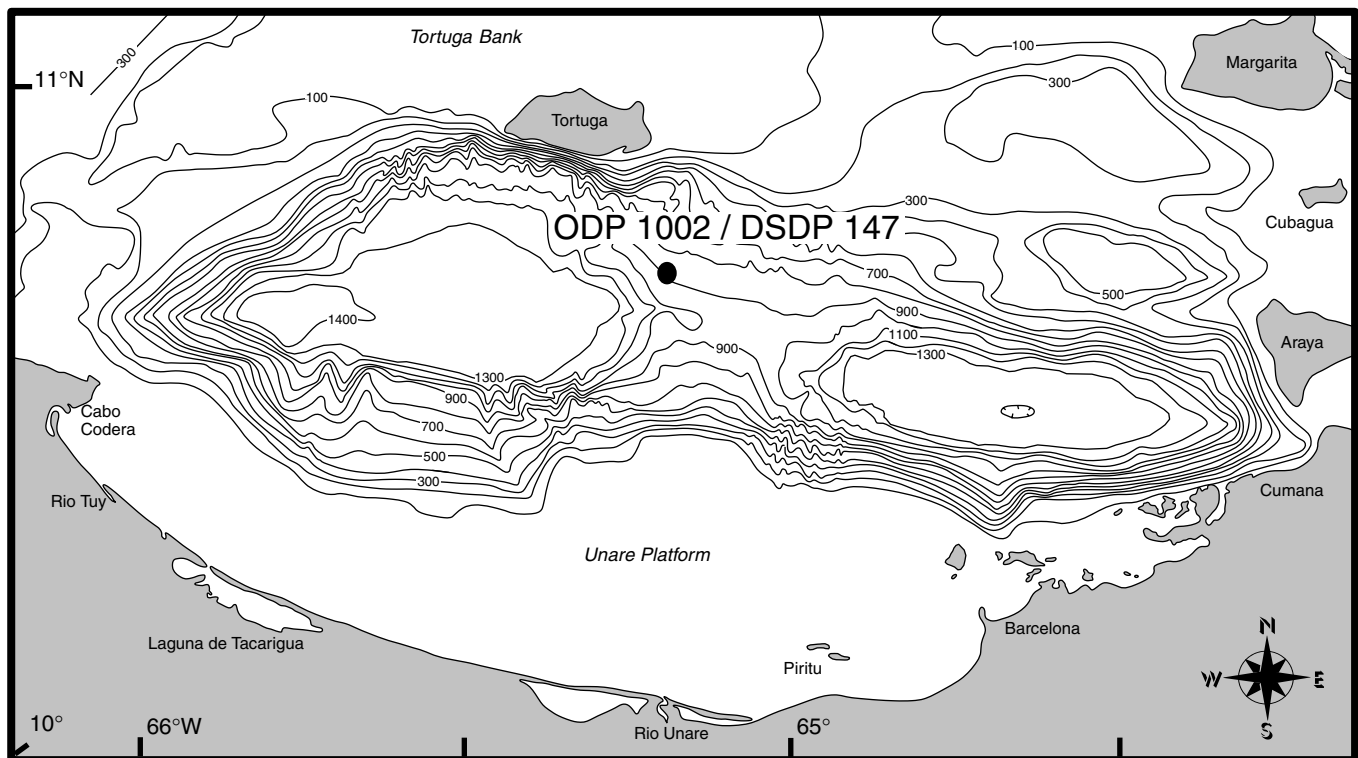


Figure 1. Bathymetric map of Cariaco Basin (in meters) showing the location of ODP Site 1002 on the western edge of the central saddle that divides the basin into two deeper sub-basins. ODP Site 1002 was drilled at almost exactly the same location as DSDP Site 147.

tral saddle. ODP Site 1002, described here, was drilled at essentially the same location (Fig. 1). The site survey for Site 1002 was conducted in 1990 on Leg 7 of the PLUME Expedition (*Thomas Washington*), which also recovered a suite of 104 box, gravity, and piston cores from all parts and depths of the basin.

In the near-surface sediment column accessible by conventional piston coring, two major sediment units are typically found. The upper unit, ranging in thickness across the basin from ~5 to 10 m, consists of dark grayish green silty clays that are generally laminated, devoid of a preserved benthic microfauna, and deposited under anoxic conditions. Laminae, where best developed in this unit, are millimeter- to submillimeter-scale in thickness and consist of light-dark sediment couplets. These couplets, preserved because of the absence of bioturbation, have been shown to reflect the strong seasonal cycle in the surface waters overlying the Cariaco Basin, with diatom and nannofossil-bearing sediment accumulation in the dry, upwelling season (winter–spring) and clay-rich accumulation in the wet, non-upwelling season (summer–fall). The interpretation of paired laminae as annual varves, at least in the most recent phase of anoxic deposition, has been confirmed by ^{210}Pb analyses and accelerator mass spectrometry (AMS) ^{14}C dating (Hughen et al., 1996a).

Beneath this anoxic unit lies a lower sediment unit composed of yellowish brown and bluish gray silty clays that are bioturbated and were clearly deposited under oxic bottom conditions. Heezen et al. (1958) originally fixed the transition between oxic and anoxic conditions in the Cariaco Basin at ~11 ka based on a single radiocarbon date of bulk organic matter. Overpeck et al. (1989) and Peterson et al. (1991) later arrived at an age of 12.6 ka for this transition based on conventional radiocarbon dates of bulk carbonate, an estimate recently confirmed by AMS ^{14}C dates on monospecific foraminiferal samples reported by Lin et al. (1997) and Hughen et al. (1998).

At the base of long piston cores, the reappearance of laminae and dark colored sediments indicate an earlier interval of deposition under anoxic conditions that ended ~26.8 ka (Lin et al., 1997). The bracketing of dates above and below the bioturbated interval suggest that oxic conditions were confined to the last glacial maximum (LGM), implying a link between deep-basin ventilation and climate that could only be investigated further through acquisition of a long, continuously cored and well-dated new record.

Results of Previous Drilling at DSDP Site 147

During DSDP Leg 15, a total of four holes were rotary drilled at Site 147 with the deepest penetration to 189 mbsf (Edgar, Saunders, et al., 1973). Hole 147 was devoted to sedimentologic and biostratigraphic studies and terminated at 162 mbsf. Holes 147A, 147B, and 147C were largely drilled for geochemical studies. The majority of cores from these latter holes were frozen, however, and never adequately described. Although a wide variety of geochemical studies of Site 147 were pursued immediately after the leg (postcruise geochemical results are published in the Leg 20 *Initial Reports of the Deep Sea Drilling Project* [Heezen, MacGregor, et al., 1973]), the sediments were largely ignored by the paleoceanographic community of that era. This is most likely a result of the perception that the rotary coring, incomplete recovery, and effects of gas (methane) expansion combined to produce a record too highly disturbed for high-resolution paleoceanographic studies.

Overall, the sedimentary section at Site 147 consisted of a grayish olive calcareous clay similar in character to that described at the top of piston cores, and largely deposited under anoxic conditions. Organic carbon content of the Holocene sediments averaged ~4 wt%, whereas samples from the late Quaternary section gave organic carbon values averaging ~1.5 wt% (ranging from <1 to 3 wt%). Sediment laminations were reported to be visible at scattered depth levels in the section, although the disruptive nature of the rotary coring used

on this early leg and the gassy nature of the sediments most likely prevented their preservation.

Rögl and Bolli (1973) and Hay and Beaudry (1973) summarized the foraminiferal and calcareous nannofossil zonations of DSDP Site 147, respectively. By current standards, the age models developed for this site were very poor. Rögl and Bolli (1973) attempted to apply the *Globorotalia menardii* zonation scheme of Ericson and Wollin (1968) and concluded that sediments at the base of Hole 147 (162 mbsf) lie within the lower V zone of these authors. Extrapolation of sedimentation rates derived from the upper part of the section led them to assign an age of ~320 ka to the base of this hole. Hay and Beaudry (1973), on the other hand, reported the first occurrence (FO) of *Emiliania huxleyi* (248 ka; Shipboard Scientific Party, 1997a) between Cores 7 and 8 (~50–60 mbsf), and tentatively identified the last occurrence (LO) of *Pseudoemiliania lacunosa* (458 ka; Thierstein et al., 1977) just above the base of Hole 147 at 162 mbsf. Although their identification of the latter datum appears to contradict the basal age estimate of Rögl and Bolli (1973), the tabulation of nannofossil data by Hay and Beaudry for the one deeper core available (i.e., not frozen) from Hole 147C shows no *P. lacunosa* present in the interval between 170 and 180 mbsf, suggesting the possibility of reworking. Hence, the question of how long a record the Cariaco Basin would yield was unresolved at the time of Leg 165 reoccupation of this location.

Site 1002

Site 1002 is located at $10^{\circ}42.37'\text{N}$, $65^{\circ}10.18'\text{W}$ on the western edge of the Cariaco Basin's central saddle. The site was positioned on a flat, well-stratified sediment package at a water depth of 893 m just east of DSDP Site 147. The operational plan at Site 1002 was to triple APC core the sediment section to a maximum safety-approved depth of 180 mbsf. Before commencing of normal drilling operations, Holes 1002A and 1002B were shot as mudline cores to obtain a good sediment/water interface and satisfy objectives of the shipboard geochemists. In Hole 1002C, the presence of dolomite crusts at various sub-bottom levels and the surprisingly firm nature of the fine-grained sediments at depths below ~120 mbsf caused the APC to fail to achieve full stroke. This necessitated a switch below that level to XCB coring in Holes 1002D and 1002E to improve recovery to meet site objectives.

All cores from Holes 1002A through 1002E were processed through the shipboard multisensor track for measurements of magnetic susceptibility and GRAPE values, but only cores from Hole 1002C were opened and described aboard the *JOIDES Resolution*. Cores from Holes 1002D and 1002E were immediately packed without splitting and stored under refrigerated conditions. The complete suite of cores was then shipped to the ODP Gulf Coast Repository at Texas A&M University where a special postcruise sampling party met from 28 May to 2 June 1996, to open, describe, and sample them. Postcruise analytical efforts reported here focus on the sediments in Hole 1002C.

RESULTS

The late Quaternary sediments at Site 1002 are generally dominated by terrigenous sediment components with variable biogenic contributions of nannofossils, diatoms, foraminifers (both planktonic and benthic), and pteropods. Throughout much of the sequence, the presence of aragonite pteropods is indicative of the generally excellent preservation of calcareous microfossils. Much of the sediment at Site 1002 is laminated, indicating deposition under nearly anoxic conditions (Fig. 2). Nevertheless, significant subsurface intervals showing clear evidence of bioturbation testify to a history of oscillation between oxic and anoxic environments in the deep basin. Because no

major changes in bulk sediment composition occur over the interval drilled, the sediments at Site 1002 were assigned to one formal lithologic unit and the eight subunits illustrated in Figures 2 and 3.

The sedimentary sequence at Site 1002 essentially duplicates the section recovered at DSDP Site 147 at virtually the same location in the central Cariaco Basin. However, in terms of recovery and core quality, there is almost no comparison between the two drilling efforts. Whereas Site 147 cores were so badly disturbed that subsurface laminae were only rarely found preserved, the APC and XCB cores from Site 1002 reveal a sequence that is intermittently laminated over much of its length.

Although cores from DSDP Site 147 were disturbed, thin layers of distinct yellowish brown and bluish gray clays similar to what were found near the surface were also identified at several deeper levels in the section (Fig. 3). The DSDP Leg 15 scientists (Edgars, Saunders, et al., 1973) postulated that these deeper clays represented earlier periods of oxic conditions comparable to those recorded during the LGM. They further suggested that sedimentation patterns in the Cariaco Basin followed a “rhythmic” alternation (Fig. 3) between periods of oxic and anoxic conditions that were related to the glacial-interglacial cycles of the late Quaternary. The lack of good biostratigraphic datums over the time interval represented by the sediments, however, effectively prevented their association of these “rhythms” with specific climatic events.

As already noted, the tentative identification of *Emiliana huxleyi* in core catchers at the base of Hole 1002C, a species that, under shipboard conditions, is difficult to distinguish from small specimens of *Gephyrocapsa* with etched central area bridges, initially led us to believe that the sedimentary sequence recovered during Leg 165 was no older than 248 ka. Indeed, the great visual similarity between the very colorful and distinctive bioturbated clays of Subunits IB and IG, and the abrupt transition to the laminated, diatom-rich anoxic sediments of overlying Subunits IA and IF, respectively, led to speculation (Shipboard Scientific Party, 1997b) that the Subunit IG-IF transition at ~98 mbsf in Site 1002 recorded the rapid deglaciation and sea level rise at ~128 ka associated with the change from marine isotope Stage (MIS) 6 to MIS 5. Shipboard observations of *Globorotalia tumida flexuosa* in the core catcher of Core 165-1002C-8H, but no higher, tended to support this hypothesis because the last occurrence datum for this taxon (80 ka) approximates the end of MIS 5. Our working model that the Subunit IG/IF boundary at ~98 mbsf corresponded to the MIS 6/5 deglaciation appeared to be further consistent with estimates based on sedimentation rates derived from an assumed sequence age of <248 ka, and with knowledge that the lithologically identical Subunit IB/IA transition was already known (e.g., Peterson et al., 1991) to coincide with the most recent deglaciation (MIS 2/1). It also seemed to fit the Leg 15 proposition that the repetitive sequence of lithologies in DSDP Site 147 reflected sedimentation cycles somehow linked to climate (Fig. 3). Postcruise efforts, however, have shown this preliminary age model to be in error as new data from shore-based stable isotope stratigraphy and biostratigraphic studies have become available.

Stable Isotope Stratigraphy and Biostratigraphic Datums

Samples for stable isotope analysis were initially taken at a frequency of one sample per 1.5-m section from all cores in Hole 1002C except Core 165-1002C-9H. Much of Core 9H was disturbed during recovery when the wireline broke and the APC barrel fell back to the bottom of the hole. To avoid including samples from this disturbed interval (~76 to 84.4 mbsf), samples were taken from Hole 1002D and spliced into the sequence from Hole 1002C. Once a preliminary stratigraphy was available at this resolution, additional samples with an average spacing of 10–30 cm and 40–60 cm were obtained from Hole 1002C that spanned the intervals that were determined to include MISs 2–4 and MIS 5, respectively. Data presented here were

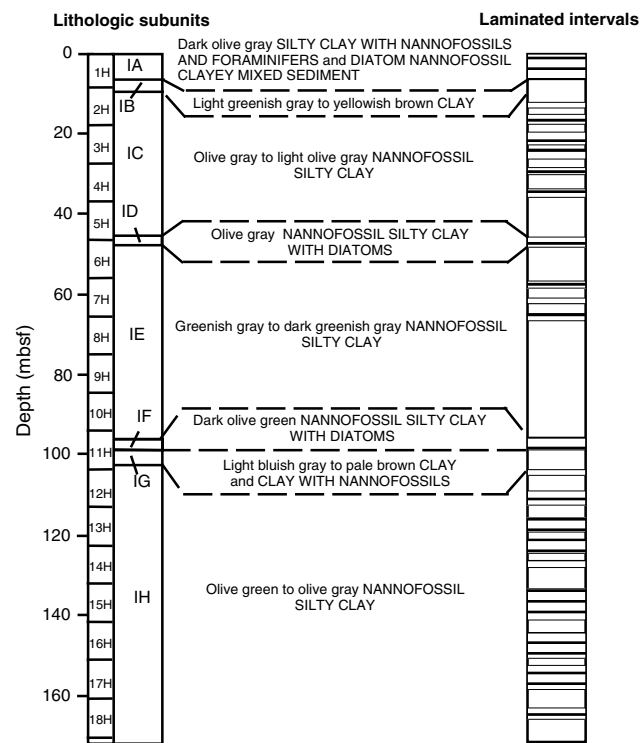


Figure 2. Simplified stratigraphic column for ODP Hole 1002C showing the subsurface distribution of defined lithologic subunits and laminated sediment intervals.

obtained from measurements on specimens of the shallow, mixed-layer dwelling planktonic foraminifer, *Globigerinoides ruber* (250–355 µm). Only specimens of the white morphotype of *G. ruber* were analyzed because Lin et al. (1997) found systematic isotopic differences between the white and pink forms of this taxon in the Cariaco Basin. All isotope analyses were made on a Finnigan-MAT 251 mass spectrometer in the Stable Isotope Laboratory of the Rosenstiel School at the University of Miami. Isotope data are reported (Table 1) in units of parts per thousand (‰) relative to the PeeDee belemnite (PDB) standard.

The δ¹⁸O data for *G. ruber* in Hole 1002C are plotted in Figure 4 together with selected biostratigraphic datums. Because of gas expansion in the core liners that occurred as cores were brought to the surface, recovery in the APC-cored Hole 1002C averaged 109.1%. To correct for this, gas voids in excess of 2 cm thick were subtracted from the sediment column and a linear compression was applied to each 1.5-m core section so that the compressed core length was equal to the actual interval cored (Piper and Flood, 1997). Hence, data in Figure 4 are plotted vs. this “corrected mbsf.”

The δ¹⁸O record for Hole 1002C can be easily matched to the well-known late Quaternary signal (e.g., Emiliani, 1955) down to about the MIS 14/13 boundary. The identification of isotope stages is consistent with a refined biostratigraphic framework largely anchored by the classic Ericson zonation scheme (Ericson et al., 1961; Ericson and Wollin, 1968). The latter is based on recognition of ecostratigraphic zones in the tropical Atlantic Ocean defined by the presence or absence of *Globorotalia menardii* and *Globorotalia tumida*. Also identified in Hole 1002C are the revised FO of the calcareous nannofossil *Emiliana huxleyi*, the LO of *Pseudoemiliana lacunosa* in MIS 12, and the disappearance of the planktonic foraminifer *Pulineniatina obliquiloculata* within the Ericson Y zone (*Y_{P. obliqu.}*). The regional disappearance of *P. obliquiloculata* is time-transgressive within the western tropical Atlantic and Caribbean and has been

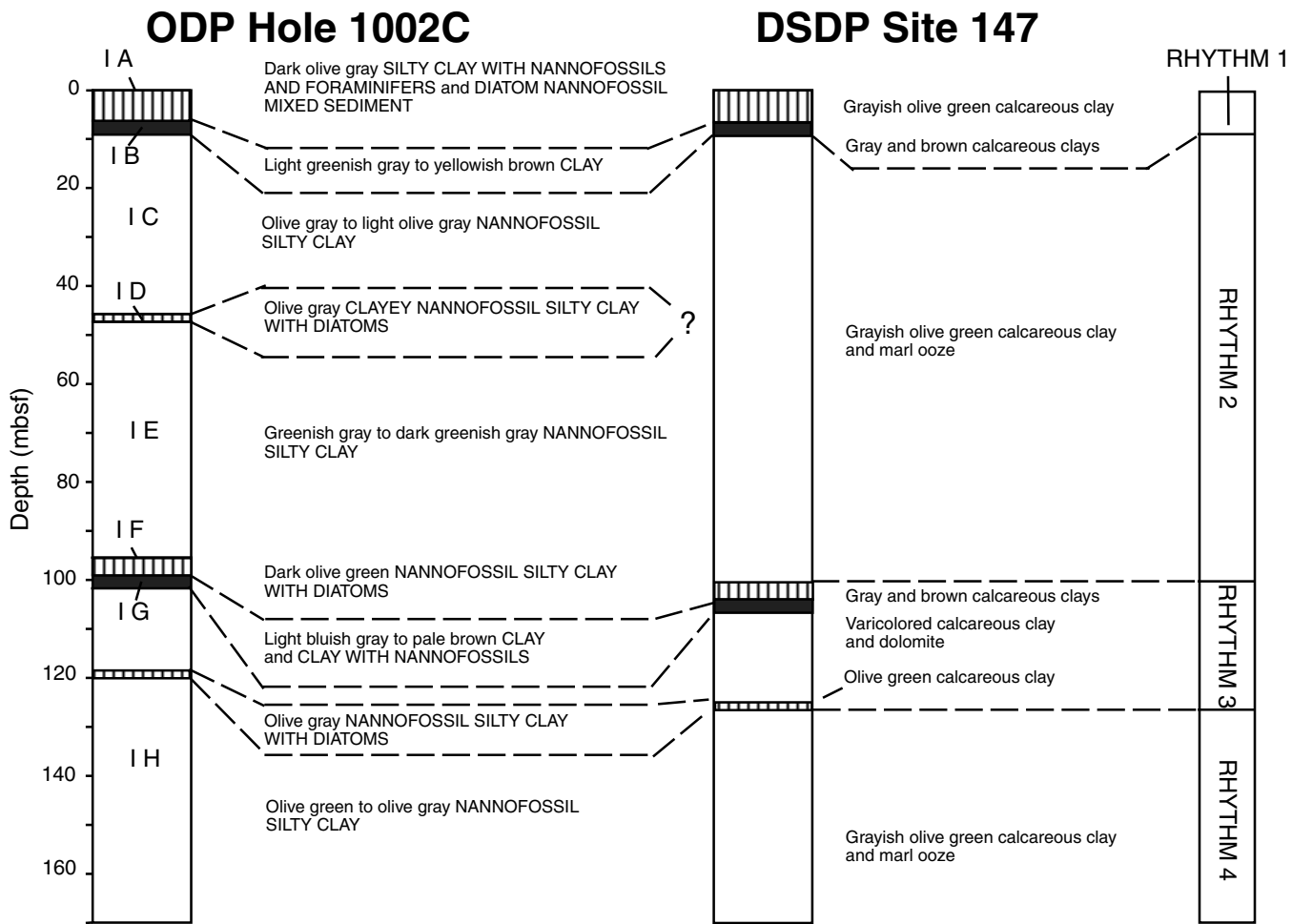


Figure 3. Comparison of lithologies recovered at ODP Site 1002 and DSDP Site 147 at approximately the same location, but separated by 26 yr of drilling technology. At both sites a virtually identical sediment sequence was recovered, although the rotary-cored Hole 147 was highly disturbed with little preserved evidence of sediment laminations. The diatom-rich interval centered at ~118 mbsf at ODP Site 1002 was missed in original core descriptions and was not formally defined as a subunit. The scientific party of DSDP Leg 15 identified a rhythmic pattern of sedimentation at Site 147, which was postulated to reflect late Quaternary glacial–interglacial cycles of climate and sea level. The available stratigraphic framework for that site, however, was never sufficient to evaluate that hypothesis.

placed between 44 and 36 ka by Prell and Damuth (1978). Biostratigraphic datums used to constrain the $\delta^{18}\text{O}$ stratigraphy are listed in Table 2.

Figure 5 shows an expanded view of the more detailed record presently available for MIS 1–6. The overall glacial–interglacial amplitude of the *G. ruber* $\delta^{18}\text{O}$ signal, both here and in the remainder of the record (Fig. 4) is large, typically well in excess of 2‰. This amplitude is similar to that previously reported by Lin et al. (1997) for this taxon for the last deglaciation. In theory, residual differences between the amplitude of the Cariaco Basin $\delta^{18}\text{O}$ signal and the change in mean ocean $\delta^{18}\text{O}$ composition expected from meltwater addition during deglaciation (~1.2‰–1.3‰; Fairbanks, 1989) should be attributable to local temperature and/or salinity effects. If solely ascribed to temperature, the residuals could represent as much as 4°–6°C of cooling of glacial surface waters over the Cariaco Basin, assuming a temperature: $\delta^{18}\text{O}$ relationship of 0.22‰ per 1°C (Epstein et al., 1953). In an earlier analysis of planktonic foraminiferal assemblages, Peterson et al. (1991) found no clear evidence of glacial cooling in the Cariaco Basin. However, these authors also noted the selective exclusion of deeper dwelling taxa from the basin during sea-level lowstands, mak-

ing quantitative SST estimates (i.e., by transfer functions) highly suspect. More recently, Lin et al. (1997) interpreted $\delta^{18}\text{O}$ data from *G. ruber* for the last glacial and reduced $\delta^{18}\text{O}$ differences among the multiple taxa analyzed to indicate glacial cooling over the Cariaco Basin of up to ~4°C. Herbert and Schuffert (Chap. 16, this volume), on the other hand, provide intriguing alkenone paleotemperature data from Hole 1002C sediments which show little cooling, if any, during the LGM and during MIS 6, but variations of up to 4°C in the earlier part of MIS 3, in MIS 4, and the later part of MIS 5. Interpreted at face value, these data would suggest that salinity variations must, at times, have played a substantial role in producing the large amplitude of the Cariaco Basin isotopic signal.

As will be discussed later in more detail, the Cariaco Basin would have been considerably more isolated during maximum sea level lowstands, likely resulting in higher salinities through basin restriction and increased evaporation. For the LGM, where alkenone data suggest little temperature change, Herbert and Schuffert (this volume) conclude that a salinity increase of ~2‰ would be required to explain the ~1‰ residual enrichment in foraminiferal $\delta^{18}\text{O}$. Support for such a salinity increase can indeed be found in foraminiferal data. Peterson

Table 1. Oxygen isotope data from ODP Hole 1002C.

Core, section, interval (cm)	Depth (mbsf)	Corrected (mbsf)	Age (ka)	¹⁸ O (‰)	Core, section, interval (cm)	Depth (mbsf)	Corrected (mbsf)	Age (ka)	¹⁸ O (‰)
165-1002C-					3H-2, 127	20.67	20.54	33.51	0.03
1H-1, 75	0.75	0.75	2.00	-1.39	3H-2, 145	20.85	20.72	33.85	-0.58
1H-2, 57	2.07	2.07	4.95	-1.28	3H-3, 17	21.07	20.93	34.24	-0.26
1H-2, 75	2.25	2.25	5.35	-1.33	3H-3, 27	21.17	21.02	34.41	0.03
1H-3, 17	3.17	3.17	7.41	-1.45	3H-3, 74	21.64	21.47	35.26	0.19
1H-3, 37	3.37	3.37	7.86	-1.37	3H-3, 97	21.87	21.69	35.67	0.45
1H-3, 75	3.75	3.75	8.71	-1.48	3H-3, 107	21.97	21.79	35.86	0.33
1H-3, 97	3.97	3.97	9.20	-1.54	3H-3, 117	22.07	21.88	36.03	-0.17
1H-3, 117	4.17	4.17	9.65	-1.43	3H-3, 127	22.17	21.98	36.22	0.44
1H-4, 17	4.67	4.67	10.76	-1.17	3H-3, 137	22.27	22.07	36.38	-0.79
1H-4, 37	4.87	4.87	11.21	-1.52	3H-4, 7	22.50	22.29	36.80	0.15
1H-4, 57	5.07	5.07	11.66	-0.76	3H-4, 17	22.60	22.39	36.99	0.65
1H-4, 75	5.25	5.25	12.06	0.01	3H-4, 27	22.70	22.48	37.15	0.67
1H-4, 97	5.47	5.47	12.55	-0.10	3H-4, 37	22.80	22.58	37.34	0.77
1H-4, 117	5.67	5.67	13.00	0.39	3H-4, 47	22.90	22.67	37.51	0.82
1H-4, 137	5.87	5.87	13.45	0.36	3H-4, 56	22.99	22.76	37.68	0.59
1H-5, 17	6.17	6.07	13.90	-0.27	3H-4, 67	23.10	22.86	37.87	0.65
1H-5, 37	6.37	6.37	14.57	0.43	3H-4, 74	23.17	22.93	38.00	0.38
1H-5, 57	6.57	6.57	14.87	0.50	3H-4, 87	23.30	23.06	38.42	0.15
1H-5, 75	6.75	6.75	15.08	0.12	3H-4, 97	23.40	23.15	38.71	0.23
1H-5, 97	6.97	6.97	15.34	-0.03	3H-4, 107	23.50	23.25	39.03	0.39
1H-5, 117	7.17	7.17	15.58	0.06	3H-4, 117	23.60	23.34	39.32	-0.37
1H-5, 137	7.37	7.37	15.82	0.09	3H-4, 137	23.80	23.53	39.94	0.40
1H-6, 17	7.67	7.67	16.17	-0.09	3H-4, 144	23.87	23.60	40.16	0.55
1H-6, 32	7.82	7.82	16.35	-0.32	3H-5, 17	24.10	23.82	40.87	-0.26
1H-6, 34	7.84	7.84	16.38	-0.44	3H-5, 37	24.30	24.01	41.49	0.30
1H-6, 57	8.07	8.07	16.65	0.48	3H-5, 47	24.40	24.11	41.81	0.45
2H-1, 17	8.57	8.57	17.07	0.71	3H-5, 57	24.50	24.20	42.10	0.26
2H-1, 37	8.77	8.76	17.18	0.27	3H-5, 67	24.60	24.30	42.42	0.35
2H-1, 57	8.97	8.96	17.30	0.53	3H-5, 74	24.67	24.36	42.62	0.12
2H-1, 74	9.14	9.12	17.40	0.54	3H-5, 87	24.80	24.49	43.04	-0.16
2H-1, 97	9.37	9.35	17.53	0.70	3H-5, 97	24.90	24.58	43.33	0.75
2H-1, 117	9.57	9.54	17.65	0.78	3H-5, 107	25.00	24.68	43.65	0.31
2H-1, 137	9.77	9.74	17.76	0.62	3H-5, 117	25.10	24.77	43.94	0.73
2H-2, 17	10.07	10.03	17.94	0.33	3H-5, 127	25.20	24.87	44.27	-0.11
2H-2, 37	10.27	10.23	18.05	1.01	3H-5, 137	25.30	24.97	44.59	-0.47
2H-2, 57	10.47	10.42	18.17	0.86	3H-6, 7	25.53	25.19	45.30	-0.66
2H-2, 74	10.64	10.59	18.27	0.72	3H-6, 17	25.63	25.28	45.59	-0.10
2H-2, 97	10.87	10.81	18.40	0.67	3H-6, 27	25.73	25.38	45.91	0.81
2H-2, 117	11.07	11.01	18.52	0.32	3H-6, 37	25.83	25.47	46.20	0.26
2H-2, 137	11.27	11.20	18.63	0.62	3H-6, 47	25.93	25.57	46.53	0.14
2H-3, 17	11.57	11.50	18.80	0.43	3H-6, 67	26.13	25.76	47.14	0.97
2H-3, 37	11.77	11.69	18.92	0.33	3H-6, 87	26.33	25.95	47.75	0.48
2H-3, 57	11.97	11.89	19.04	0.59	3H-6, 97	26.43	26.04	48.04	0.49
2H-3, 74	12.14	12.05	19.13	0.76	3H-6, 107	26.53	26.14	48.37	0.69
2H-3, 97	12.37	12.28	19.27	0.74	3H-6, 117	26.63	26.24	48.69	0.46
2H-3, 117	12.57	12.47	19.38	0.58	3H-6, 127	26.73	26.33	48.98	0.46
2H-3, 137	12.77	12.67	19.50	0.85	3H-6, 137	26.83	26.43	49.30	0.47
2H-4, 17	13.07	12.96	19.67	0.41	3H-6, 146	26.92	26.51	49.56	0.97
2H-4, 37	13.27	13.16	19.79	0.44	3H-7, 7	27.03	26.62	49.92	0.87
2H-4, 57	13.47	13.35	19.90	0.46	3H-7, 16	27.12	26.72	50.24	0.91
2H-4, 74	13.64	13.52	20.00	0.83	3H-7, 37	27.33	26.90	50.82	0.75
2H-4, 97	13.87	13.74	20.43	0.41	3H-7, 47	27.43	27.00	51.15	0.29
2H-4, 117	14.07	13.94	20.82	0.52	3H-7, 57	27.53	27.09	51.44	0.88
2H-4, 137	14.27	14.13	21.19	-0.26	3H-1, 7	27.47	27.47	52.66	0.57
2H-5, 17	14.57	14.42	21.76	0.11	3H-1, 17	27.57	27.56	52.95	0.88
2H-5, 37	14.77	14.62	22.15	0.38	4H-1, 37	27.77	27.75	53.57	0.35
2H-5, 57	14.97	14.81	22.52	0.08	4H-1, 47	27.87	27.85	53.89	1.08
2H-5, 74	15.14	14.98	22.85	0.21	4H-1, 57	27.97	27.94	54.18	0.88
2H-5, 97	15.37	15.21	23.30	0.36	4H-1, 74	28.14	28.10	54.70	-0.07
2H-5, 117	15.57	15.40	23.67	0.15	4H-1, 83	28.23	28.19	54.99	0.42
2H-5, 137	15.77	15.60	24.06	-0.50	4H-1, 105	28.45	28.40	55.67	-0.05
2H-6, 17	16.07	15.89	24.62	0.39	4H-1, 127	28.67	28.61	56.35	0.64
2H-6, 37	16.27	16.08	24.99	0.56	4H-1, 137	28.77	28.70	56.64	1.12
2H-6, 57	16.47	16.28	25.38	0.29	4H-1, 147	28.87	28.80	56.96	0.67
2H-6, 74	16.64	16.45	25.72	0.18	4H-2, 7	28.97	28.89	57.25	0.13
2H-6, 97	16.87	16.67	26.15	0.06	4H-2, 17	29.07	28.99	57.57	-0.09
2H-6, 117	17.07	16.87	26.54	-0.74	4H-2, 27	29.17	29.08	57.86	-0.12
2H-6, 137	17.27	17.06	26.91	-0.01	4H-2, 37	29.27	29.18	58.19	0.83
2H-7, 17	17.57	17.35	27.47	-0.02	4H-2, 47	29.37	29.27	58.48	0.99
2H-7, 22	17.62	17.40	27.57	-0.27	4H-2, 74	29.64	29.53	59.32	0.64
2H-7, 37	17.77	17.55	27.86	0.16	4H-2, 87	29.77	29.65	59.70	0.55
3H-1, 7	17.97	17.97	28.68	0.26	4H-2, 107	29.97	29.84	60.32	0.77
3H-1, 17	18.07	18.06	28.85	0.03	4H-2, 117	30.07	29.94	60.64	1.13
3H-1, 27	18.17	18.16	29.04	-0.42	4H-2, 127	30.17	30.03	60.93	1.21
3H-1, 76	18.66	18.63	29.92	-0.17	4H-2, 137	30.27	30.13	61.25	0.90
3H-1, 87	18.77	18.73	30.11	-0.16	4H-3, 17	30.60	30.44	62.26	1.04
3H-1, 127	19.17	19.11	30.82	-0.17	4H-3, 74	31.17	30.98	64.00	0.16
3H-1, 137	19.27	19.21	31.01	0.33	4H-3, 97	31.40	31.20	66.11	0.49
3H-1, 147	19.37	19.30	31.18	-0.02	4H-3, 127	31.70	31.49	67.12	1.15
3H-2, 7	19.47	19.40	31.37	0.08	4H-4, 7	32.07	31.84	68.35	1.06
3H-2, 17	19.57	19.49	31.54	0.13	4H-4, 37	32.37	32.12	69.34	0.73
3H-2, 27	19.67	19.59	31.73	-0.09	4H-4, 74	32.74	32.45	70.50	-0.77
3H-2, 37	19.77	19.69	31.91	0.41	4H-4, 87	32.87	32.60	71.14	-0.73
3H-2, 47	19.87	19.78	32.08	0.24	4H-4, 117	33.17	32.88	72.34	-0.30
3H-2, 67	20.07	19.97	32.44	-0.93	4H-5, 57	34.18	33.84	76.45	-1.34
3H-2, 74	20.14	20.04	32.57	0.11	4H-5, 71	34.32	33.97	77.00	-0.44
3H-2, 87	20.27	20.16	32.80	0.47	4H-5, 107	34.68	34.32	78.50	-0.88
3H-2, 107	20.47	20.35	33.15	0.33	4H-6, 17	35.31	34.91	81.02	-1.36

Table 1 (continued).

Core, section, interval (cm)	Depth (mbsf)	Corrected (mbsf)	Age (ka)	$\delta^{18}\text{O}$ (‰)	Core, section, interval (cm)	Depth (mbsf)	Corrected (mbsf)	Age (ka)	$\delta^{18}\text{O}$ (‰)
4H-6, 47	35.61	35.20	82.27	-0.80	10H-4, 75	88.96	88.33	291.47	-0.19
4H-6, 74	35.88	35.46	83.38	0.41	10H-5, 74	90.50	89.66	298.00	0.03
4H-7, 7	36.71	36.24	86.71	-0.80	10H-6, 73	92.06	91.00	306.34	-0.83
4H-7, 18	36.82	36.35	87.19	0.08	10H-7, 67	93.50	92.24	314.03	-0.83
4H-7, 50	37.14	36.65	88.47	-0.74	10H-8, 74	95.07	93.59	322.40	-0.37
5H-1, 27	37.17	37.15	90.61	-0.86	11H-2, 79	94.92	94.82	330.00	-1.48
5H-1, 75	37.65	37.60	92.53	-0.46	11H-3, 78	96.41	96.17	332.27	-1.16
5H-1, 97	37.87	37.80	93.39	-0.47	11H-4, 79	97.97	97.58	334.65	0.03
5H-1, 127	38.17	38.08	94.59	-1.07	11H-5, 79	99.67	99.12	337.24	0.38
5H-2, 7	38.47	38.36	95.78	0.04	11H-6, 78	101.27	100.57	339.68	-0.22
5H-2, 35	38.75	38.62	96.90	-1.36	11H-7, 78	102.80	101.95	342.00	1.03
5H-2, 67	39.07	38.92	98.18	-1.57	11H-CC, 18	104.25	103.27	347.01	0.81
5H-2, 75	39.15	39.00	98.52	-0.59	12H-1, 80	104.20	104.08	350.10	0.52
5H-2, 135	39.75	39.56	100.92	-0.59	12H-2, 73	105.40	105.10	354.00	0.73
5H-3, 17	40.07	39.86	102.20	-1.75	12H-3, 78	106.95	106.41	357.55	0.53
5H-3, 87	40.77	40.51	104.98	-1.42	12H-4, 78	108.45	107.68	360.99	-0.02
5H-3, 117	41.07	40.79	106.18	-0.42	12H-5, 78	109.95	108.95	364.43	-0.04
5H-3, 144	41.34	41.04	107.25	0.03	12H-6, 78	111.51	110.27	368.00	-0.75
5H-4, 27	41.74	41.41	108.83	-0.28	12H-7, 78	113.01	111.55	373.04	-0.20
5H-4, 75	42.22	41.86	110.76	-0.94	12H-CC, 24	114.49	112.80	378.00	-0.17
5H-4, 97	42.44	42.06	111.61	-1.80	13H-1, 74	113.64	113.55	382.86	-0.27
5H-4, 127	42.74	42.34	112.81	-1.36	13H-2, 72	114.73	114.50	389.02	-0.91
5H-5, 7	43.04	42.62	114.01	-1.43	13H-3, 92	116.43	115.99	398.64	-1.04
5H-5, 37	43.34	42.90	115.21	-1.74	13H-4, 72	117.73	117.12	406.00	-1.46
5H-5, 67	43.64	43.18	116.41	-1.08	13H-5, 72	119.23	118.43	412.57	-1.21
5H-5, 75	43.72	43.26	116.75	-1.24	13H-6, 72	120.73	119.74	419.15	-0.93
5H-5, 107	44.04	43.56	118.03	-1.16	13H-7, 72	122.23	121.06	425.75	-0.36
5H-5, 137	44.34	43.84	119.23	-0.94	14H-1, 35	122.75	122.70	434.00	0.79
5H-6, 17	44.64	44.12	120.43	-0.82	14H-2, 71	123.71	123.53	440.23	0.85
5H-6, 75	45.22	44.66	122.74	-1.00	14H-3, 72	125.22	124.84	450.05	0.85
5H-6, 117	45.64	45.05	124.41	-1.57	14H-4, 73	126.73	126.14	459.80	0.37
5H-6, 146	45.93	45.32	125.56	-0.88	14H-5, 73	128.30	127.50	470.00	0.47
5H-7, 27	46.24	45.61	126.80	-1.86	14H-6, 73	129.89	128.87	472.00	0.41
5H-7, 57	46.54	45.89	128.00	-1.16	15H-2, 74	133.31	133.12	478.20	-0.06
6H-1, 7	46.47	46.46	130.51	-0.10	15H-3, 77	134.84	134.45	480.15	-0.58
6H-2, 17	46.84	46.80	132.00	0.04	15H-4, 74	136.31	135.72	482.00	-1.17
6H-2, 47	47.14	47.07	133.19	1.08	15H-5, 74	137.81	137.02	485.96	-0.70
6H-2, 74	47.41	47.31	134.24	0.79	15H-6, 74	139.34	138.35	490.01	-0.40
6H-2, 117	47.84	47.70	135.96	0.46	15H-7, 77	140.72	139.55	493.66	-0.70
6H-2, 143	48.10	47.93	136.97	0.48	15H-8, 77	142.22	140.79	497.43	-0.48
6H-3, 73	48.90	48.65	140.13	0.38	16H-1, 40	141.80	141.75	500.35	-0.37
6H-4, 7	49.74	49.40	143.43	0.31	16H-2, 39	142.36	142.24	501.85	-0.15
6H-5, 73	51.90	51.35	152.00	0.88	16H-3, 46	143.93	143.62	506.05	-0.72
6H-7, 78	55.05	54.18	160.73	0.20	16H-4, 72	145.69	145.16	510.73	-0.27
6H-8, 78	56.55	55.53	164.89	0.19	16H-5, 74	147.21	146.50	514.81	-0.10
7H-1, 74	56.64	56.52	167.94	-0.29	16H-6, 74	148.71	147.81	518.80	-0.95
7H-2, 74	57.52	57.26	170.21	0.22	16H-7, 79	150.26	149.17	522.94	-0.55
7H-3, 79	59.07	58.55	174.20	-0.30	16H-8, 74	151.71	150.45	526.82	-0.52
7H-4, 74	60.52	59.77	177.95	-0.28	17H-1, 73	151.63	151.59	530.30	-0.01
7H-5, 74	62.09	61.08	182.00	0.69	17H-2, 73	153.21	153.07	534.81	-0.31
7H-6, 74	63.64	62.37	183.66	-0.30	17H-3, 73	154.77	154.54	539.28	-1.18
8H-3, 72	68.17	67.81	190.63	-0.47	17H-4, 73	156.35	156.03	543.82	-0.02
8H-4, 74	69.69	69.13	192.33	-0.77	17H-5, 73	157.90	157.49	548.26	-0.92
8H-5, 74	71.19	70.43	194.00	-1.11	17H-6, 73	159.40	158.90	552.55	-0.83
8H-6, 74	72.72	71.76	200.02	-0.77	17H-7, 21	160.38	159.83	555.38	-0.82
8H-7, 76	74.24	73.08	206.00	-0.19	18H-1, 73	161.13	161.10	559.25	-0.63
8H-8, 74	75.72	74.36	216.00	-0.62	18H-2, 73	162.63	162.54	563.63	-0.96
9H-1, 77	75.67	75.64	222.35	-0.21	18H-3, 73	164.13	163.97	567.99	-1.47
9H-2, 74	76.85	76.78	228.00	0.10	18H-5, 73	166.11	165.87	573.77	-0.99
9H-3, 74	78.35	78.23	238.00	-0.62	18H-6, 68	167.56	167.26	578.00	-1.08
9H-5, 74	81.35	81.13	250.00	0.48					
9H-6, 74	82.85	82.58	258.00	0.29					
9H-7, 67	84.28	83.96	270.00	0.69					
10H-1, 75	85.15	85.05	275.35	-0.12					
10H-2, 71	85.92	85.71	278.60	-0.03					
10H-3, 72	87.43	87.01	284.98	-0.92					

Notes: Data are reported in standard ‰ notation relative to PDB. All analyses are based on specimens of *Globigerinoides ruber* (250–355 µm). Estimated ages for samples were derived from correlation to the SPECMAP time scale (Imbrie et al., 1984).

et al. (1991) noted that higher glacial salinities in the Cariaco Basin could at least partially explain the dominance of *G. ruber* in LGM sediments. In addition, preliminary benthic foraminiferal census data from Hole 1002C in at least some intervals of glacial Stages 2–4 show that populations are dominated by members of the miliolid genus *Pyrgo*, which are high-Mg calcite, and by the aragonitic genus *Hoeglundina*. Both taxa are common in high salinity, carbonate-saturated environments today such as the Red Sea and Persian Gulf (e.g., Halicz and Reiss, 1981; Locke and Thunell, 1988).

Superimposed on the orbital-scale variability of the MIS 1 to 6 interval is clear evidence for millennial and submillennial variability in $\delta^{18}\text{O}$ (Fig. 5) that can probably also be attributed to local temperature and/or salinity effects. Similar high-frequency oscillations in a planktonic foraminiferal $\delta^{18}\text{O}$ record (EW9209 JPC) from the open western equatorial Atlantic have been observed by Curry and Oppo

(1997). The amplitude of the high-frequency $\delta^{18}\text{O}$ oscillations at that location, interpreted by Curry and Oppo (1997) as a temperature signal, is ~0.6‰ and are superimposed on a glacial–interglacial amplitude of ~2.1‰. Measured amplitudes of the high-frequency oscillations at Site 1002 are larger, but may be a function of the resolution afforded by the much higher deposition rates at this site. Although it is tempting to speculate that low isotopic values most evident in sediments of MIS 3 in the Cariaco Basin (Fig. 5) can be correlated to individual high-frequency events in the Curry and Oppo (1997) record from EW9209 JPC, and, in turn, to the well-known warm interstadial events in the Greenland ice core records (e.g., GRIP Members, 1993), the age control at Site 1002 is not yet robust enough to attempt this match. Furthermore, salinity effects related to potential freshwater discharge into the Cariaco Basin must also be carefully evaluated. Clear evidence of a major freshwater event in the Cariaco Basin at

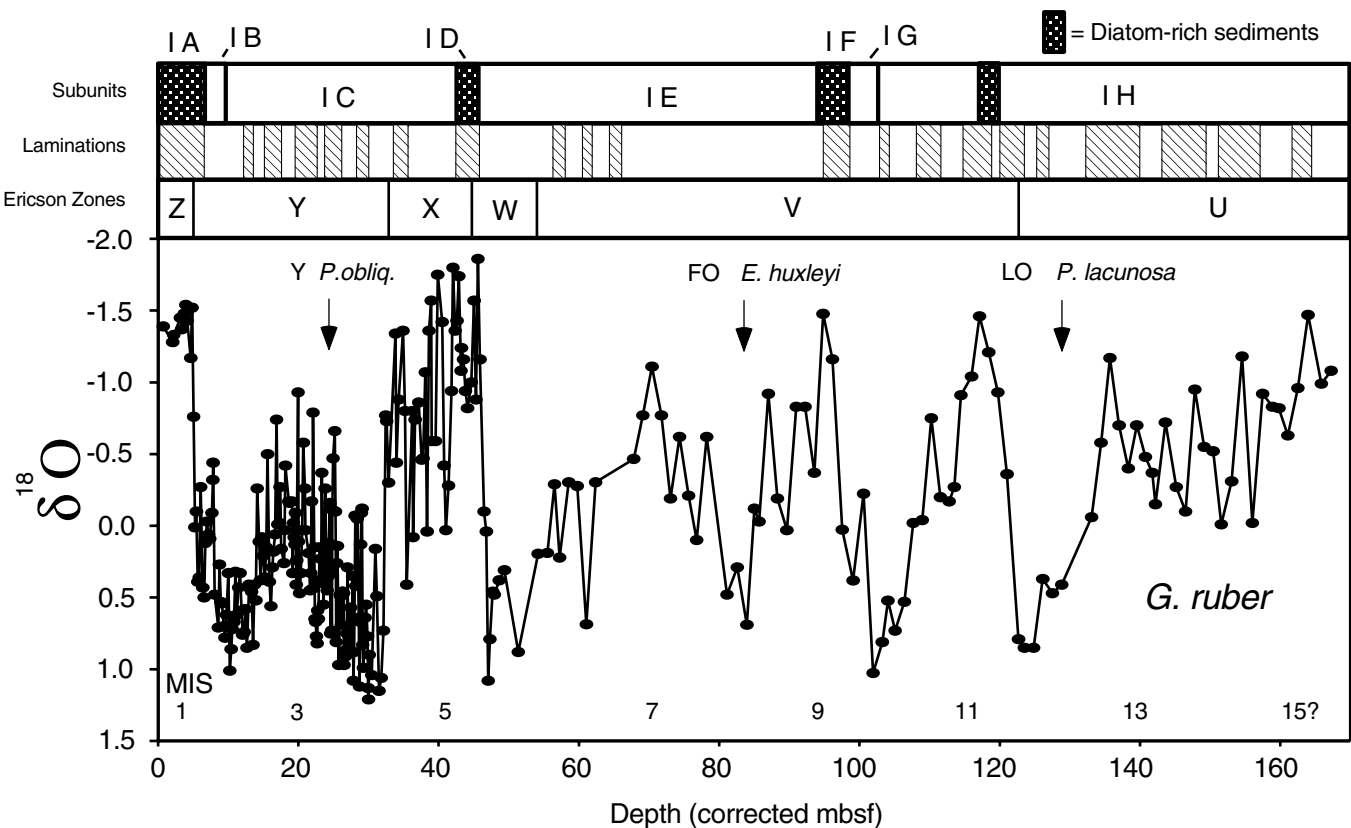


Figure 4. Oxygen isotope stratigraphy for Hole 1002C based on measurements of the shallow, mixed-layer dwelling *Globigerinoides ruber* (‰, PDB). Data are plotted against sub-bottom depths that have been corrected for voids and gas expansion (see details in text). Standard marine isotope stages (MIS) are shown across the bottom, and the historical Ericson Zones (Z, Y, X, etc.) are shown across the top. Other biostratigraphic datums are described in the text. The stratigraphic distribution of lithologic subunits and visibly laminated intervals is indicated at the top. Diatom-rich subunits include the base of Subunits IA, ID, IF, and the interval of sediment centered at ~118 mbsf. Subunits IB and IG contain distinctive bluish gray to yellowish brown clays.

Table 2. Biostratigraphic datums recognized at Site 1002.

Hole, core, section, interval (cm)	Depth (mbsf)	Event type	Species	Age (Ka)	Ericson zone
1002C-1H-4, 17	4.67	AS	<i>Globorotalia menardii/tumida</i>	9	Y/Z
1002C-3H-3, 75	21.64	AS	<i>Pulleniatina obliquiloculata</i>	~40	Y/ <i>P. obliqua</i>
1002C-4H-5, 72	34.32	AS/LO	<i>Globorotalia menardii/tumida/flexuosa</i>	80	X/Y
1002C-5H-6, 75	45.22	AS	<i>Globorotalia menardii/tumida</i>	130	W/X
1002C-6H-7, 79	55.05	AS	<i>Globorotalia menardii/tumida</i>	165	V/W
1002D-9H-8, 77	82.15	FO	<i>Emiliania huxleyi</i>	248	
1002C-13H-6, 72	120.73	AS	<i>Globorotalia menardii/tumida</i>	425	U/V
1002C-14H-CC	133.15	LO	<i>Pseudoemiliania lacunosa</i>	458	

Notes: AS = abundance shift, FO = first occurrence, LO = last occurrence. Age estimates presented here were used to help constrain the $\delta^{18}\text{O}$ stratigraphy for this site but were not used as tie points in the age model applied to Figure 6. Reported depths are in original mbsf and are not corrected for gas expansion. Ericson zones are after Ericson et al. (1961) and Ericson and Wollin (1968).

~14 ka has already been documented by Lin et al. (1997), suggesting the potential for similar events earlier in the record. The question of abrupt events and high-frequency variability in $\delta^{18}\text{O}$ and lithologic records of Site 1002 will be more fully evaluated elsewhere.

Comparison of the long $\delta^{18}\text{O}$ record in Hole 1002C with the downcore distribution of lithologic subunits leads to other interesting observations (Fig. 4). Sediments of Subunit IG, consisting of colorful interbedded light bluish gray and pale brown clays, are visually and lithologically most similar to the clays of Subunit IB that were deposited in the latter stages of MIS 2 (LGM). As noted above, it was this visual similarity that largely contributed to earlier speculation (Shipboard Scientific Party, 1997b) that the Subunit IG/IF boundary cor-

responded to the sharp deglaciation (Termination II) associated with the MIS 6/5 transition. The $\delta^{18}\text{O}$ stratigraphy for Hole 1002C, however, clearly indicates that Subunit IG was deposited much earlier, near the end of MIS 10, and that the MIS 6–5 transition actually falls at an expansion-corrected depth of ~46 mbsf. Why clays associated with the termination of glacial MIS 10 are the only other sediments at Site 1002 visually identical to the distinct yellow and gray clays of the LGM is not clear. Whatever the reason, the simple model of sedimentary “rhythms” first proposed for DSDP Site 147 (Fig. 3) is clearly more complex than originally envisioned, with individual rhythms encompassing more than one complete glacial–interglacial cycle.

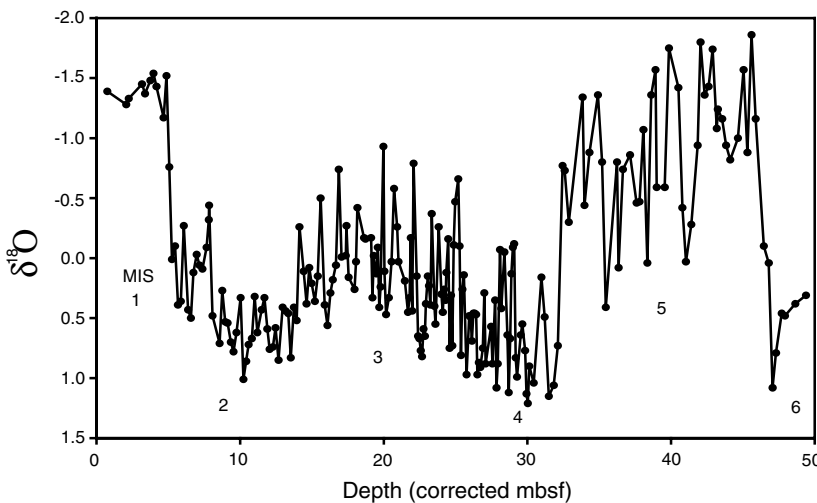


Figure 5. Expanded detail of the $\delta^{18}\text{O}$ record of *G. ruber* for MIS 1 to the top of MIS 6 in Hole 1002C. Data are plotted against sub-bottom depths that have been corrected for voids and gas expansion (see details in text).

A first-order correlation of the Hole 1002 $\delta^{18}\text{O}$ record to the SPECMAP composite standard for the late Quaternary (Imbrie et al., 1984) is shown in Figure 6. Although resolution of the Hole 1002C record is relatively low below MIS 5 because of the wide sampling interval (1 sample/section) currently used, filtered comparisons of the Site 1002 and SPECMAP $\delta^{18}\text{O}$ records in the orbital bands of precession and obliquity indicate that the two records are well matched in the time domain (Fig. 7). The present age model (Fig. 8) indicates a basal age of ~580 ka for the recovered Cariaco Basin sequence, yielding an average sedimentation rate of ~35 cm/k.y. (350 m/m.y.). This rate is similar to previous estimates of sedimentation for the uppermost sequence (Peterson et al., 1991; Hughen et al., 1996b; Lin et al., 1997).

Diatom-rich sediments are characteristic of the well-laminated lower portion of Subunit IA, as well as being the diagnostic criterion used to define Subunits ID and IF. Shore-based examination of smear slides has also identified a diatom-rich interval centered on ~118 mbsf (Figs. 3, 4) that was initially missed and not given subunit status. Interestingly, all intervals rich in biogenic opal correspond to times of peak interglacial conditions (MIS 1, 5e, 9, and 11) immediately following abrupt glacial terminations. The implications of this observation are discussed below. Biogenic opal measurements that are not yet complete should soon provide a more rigorous and complete picture of opal deposition patterns in the Cariaco Basin over the past 580 ka.

Calcium Carbonate and Organic Carbon Deposition

Calcium carbonate and total organic carbon (TOC) data are presented in Figure 9. Measurements of carbonate and TOC were made at the University of British Columbia (by GHH) on samples spaced at ~30-cm intervals in Hole 1002C. The calcium carbonate content of the sediments was measured coulometrically, whereas percent TOC was derived from the difference between total carbon (analyzed using a Carlo-Erba CHN analyzer) and carbonate carbon. Analytical precision for the TOC and carbonate data is ± 1.2 wt% and ± 2 wt%, respectively.

The TOC and carbonate data from the Cariaco Basin show a strong relationship with the planktonic foraminiferal $\delta^{18}\text{O}$ record (Fig. 9). Although clear exceptions exist, sediments deposited during interglacial periods are generally characterized by both high TOC and carbonate contents. Interglacial TOC values range from averages of ~3 wt% in MIS 5, 7, 9, and 13, to as much as 5 wt% in MIS 1 and 11, whereas glacial TOC contents are as low as 0.1–1.3 wt%. In a similar fashion, the carbonate contents of interglacial sediments typically increase to between 20 and 40 wt%, whereas glacial carbonate

values are generally less than 10 wt%. Superimposed on this glacial-interglacial pattern is evidence of higher frequency variability in both measured proxies; short-term TOC fluctuations, for example, are especially pronounced in MIS 3 sediments in a pattern similar to that observed in the record of $\delta^{18}\text{O}$ (Fig. 5).

The organic component of the Cariaco Basin sediments is thought to be predominantly of marine origin, although a minor terrigenous component may be present (Haug et al., 1998). Wakeham and Ertel (1988) reported $\delta^{13}\text{O}$ values of about $-20\text{\textperthousand}$ for the organic fraction of Holocene box core sediments, values typical of those observed in subtropical phytoplankton (Rau, 1994). In an analysis of eight depth-distributed samples from the old DSDP Site 147, McIver (1973) reported an average $\delta^{13}\text{O}$ of $-21.0\text{\textperthousand}$ for bulk organic matter, with values ranging from $-20.4\text{\textperthousand}$ to as light as $-22.25\text{\textperthousand}$ in one sample at 62 mbsf. McIver (1973) interpreted the latter value to reflect a modest increase in terrigenous contributions to the basin during a period of sea-level lowstand. To the extent that sub-bottom depths in Sites 1002 and 147 appear to be comparable (e.g., Fig. 2), this particular sample may have been deposited during MIS 6.

Coccoliths and foraminifers are the dominant source of biogenic carbonate in sediments of the Cariaco Basin, with small but significant contributions from pteropods (aragonite) over much of the sequence. Benthic foraminifers, ostracodes, and micromollusks in the >150-mm size fraction are present or largely absent as a function of the ventilation history of the basin, but probably do not contribute much to the total carbonate budget of the sediments. Although turbidite deposition appears to be minimal at the Site 1002 location on the Cariaco Basin's flat central saddle, the occasional presence of micro-turbidites (subcentimeter sized), molluscan debris, and abraded benthic foraminifers from the surrounding shelf in samples indicates the likely sporadic introduction of reworked materials into the sediment. The presence of reworked shelf carbonate may account for scattered high carbonate values (e.g., during MIS 8) that rise above the background pattern of carbonate variability (Fig. 9).

Terrigenous Matter Deposition

The abundance of terrigenous matter (weight percent) in the bulk sediment was calculated at a sampling interval of ~2 samples/1.5 m core section (Fig. 9) using a Ti-based normative calculation:

$$\% \text{ terrigenous matter} = (\text{Ti}_{\text{sample}} / \text{Ti}_{\text{PAAS}}) \times 100.$$

Concentrations of Ti were measured (by KMY and RWM) using ICP-emission spectrometry (ICP-ES) at Boston University, utilizing

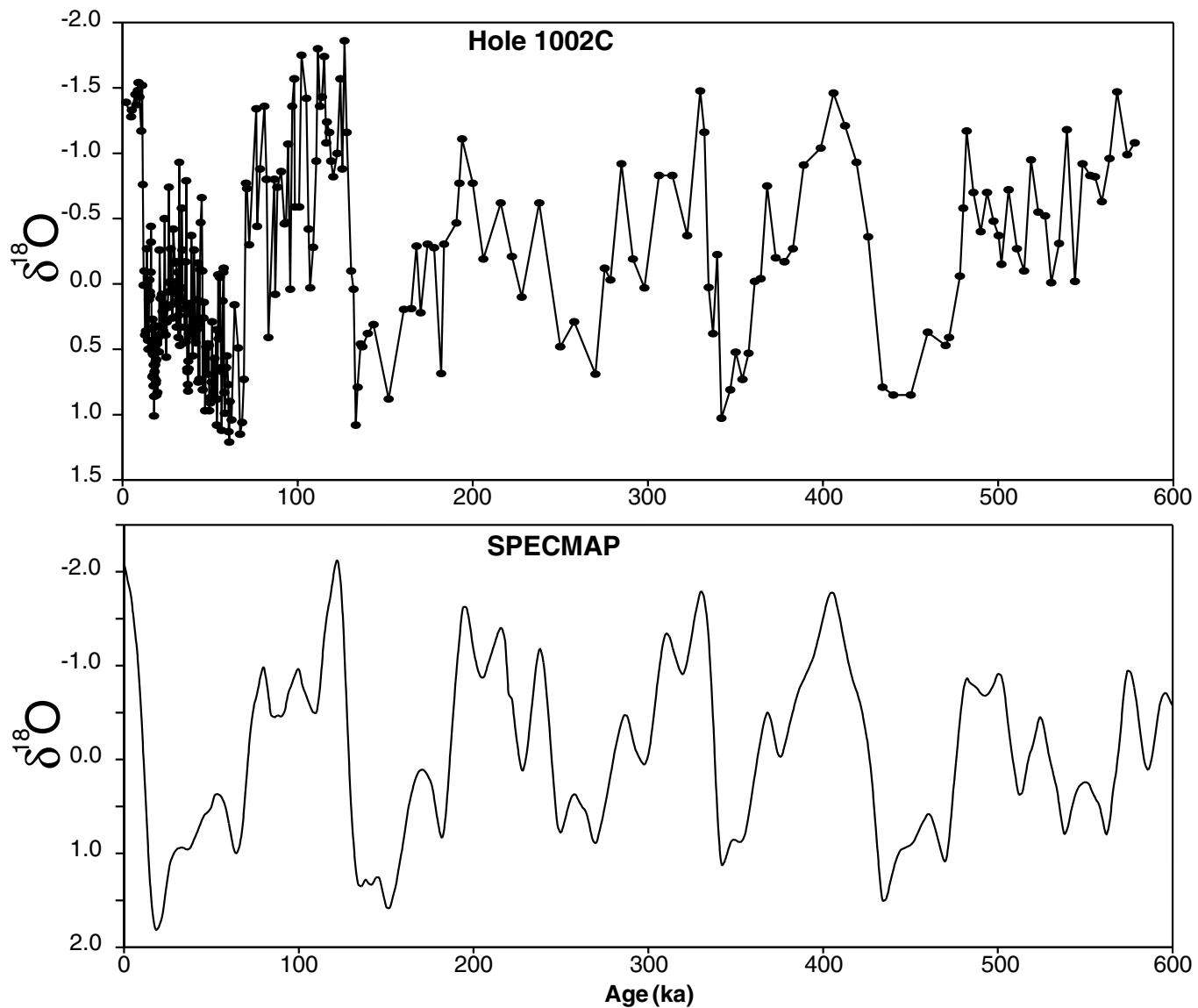


Figure 6. Comparison between the $\delta^{18}\text{O}$ record of Hole 1002C and the standard SPECMAP composite record (expressed in standard deviation units; Imbrie et al., 1984), with both plotted using the SPECMAP time scale. Despite the low resolution of the Hole 1002C record below MIS 5 (1 analysis/core section), the well-known pattern of $\delta^{18}\text{O}$ variation for the late Quaternary can clearly be seen. Application of the SPECMAP time scale indicates a basal age of ~580 ka for the Cariaco Basin sediments recovered at Site 1002.

a suite of International Standard Reference Materials to assure precision (~2% of the measured value) and accuracy (within precision). This calculation assumes that terrigenous matter in the Cariaco Basin is similar chemically to Post-Archean Average Shale (PAAS) (Taylor and McLennan, 1985). While it is possible that this is not the case, PAAS is commonly used as a reference point for comparisons to other sediment. Furthermore, it has been shown that Ti concentrations in different “average shales” do not vary significantly (Murray and Leinen, 1993, 1996). Our normative calculation also assumes that all of the Ti in the sediment is mineralogically tied up in the terrigenous component. Though Ti is relatively particle reactive, variations in terrigenous matter using this equation cannot be attributed to adsorption by biogenic matter (e.g., Murray and Leinen, 1996) because such a biogenically scavenged component can only be detected in systems where biogenic matter comprises >95 wt% of the bulk sediment (Murray and Leinen, 1996). Titanium also does not respond to redox variations (Taylor and McLennan, 1985), so Ti variations in Cariaco

Basin sediments are not diagenetically controlled. Thus, results shown in Figure 9 represent maximum estimates of the terrigenous contribution to each sample.

The Ti-based normative calculation indicates that the terrigenous matter content of Site 1002 sediments ranges from 36 to 91 wt% of the total bulk composition, with an average contribution of 63 wt% $\pm 11\%$. In general, the terrigenous contents of the sediments appear to have been high during glacial intervals and low during interglacials, a pattern perhaps not unexpected in a hemipelagic environment where climate and sea-level change are likely to have markedly affected sediment deposition.

DISCUSSION

The $\delta^{18}\text{O}$ stratigraphy and biostratigraphic datums reported here indicate a late Quaternary sequence at Site 1002 that is considerably

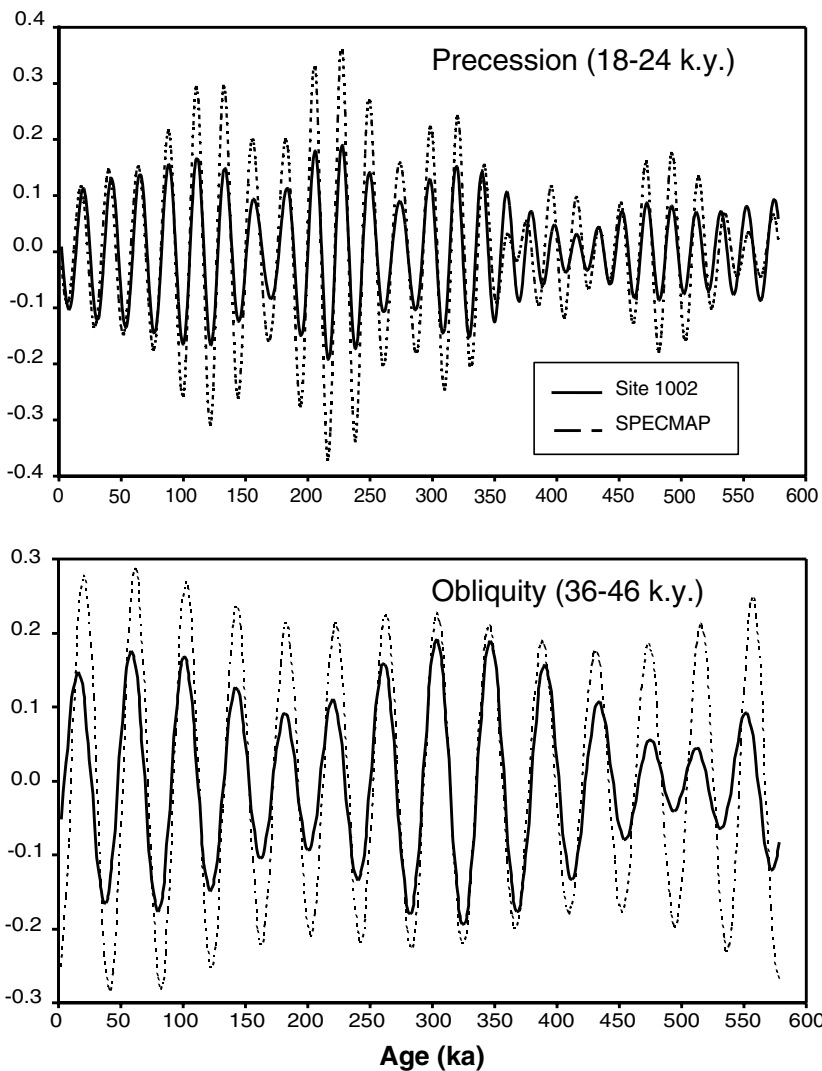


Figure 7. Comparison of filtered components of the Site 1002 and SPECMAP $\delta^{18}\text{O}$ records corresponding to the frequencies of precession (top; filter centered at 21 k.y.) and obliquity (bottom; filter centered at 41 k.y.). All curves have been transformed to have zero means with arbitrary scales. Inspection of the filtered data show that the isotopic signals of Site 1002 are well matched to the SPECMAP $\delta^{18}\text{O}$ chronology in both frequency bands.

older than what was initially thought when the “Site 1002” chapter of the *Initial Reports* volume was prepared and published (Shipboard Scientific Party, 1997b). Correlation of the $\delta^{18}\text{O}$ record to the SPECMAP standard now suggests a basal age for Site 1002 of ~580 ka, terminating in sediments deposited at about the MIS 15/14 boundary. Time series of tropical ocean and climate variability presently being generated from this site will provide important comparisons to other high-resolution records and should yield new insights into tropical climate processes and extra-tropical teleconnections.

As previously noted, Leg 15 scientists postulated that the rhythmic pattern of facies variations recorded in DSDP Site 147 sediments is the result of large-scale changes in climate and sea level associated with recent glacial-interglacial cycles. The correlations observed between the $\delta^{18}\text{O}$ record in Hole 1002C and the relative proportions of carbonate, TOC, and terrigenous material (Fig. 9), plus the regular appearance of diatom-rich intervals (Fig. 4), clearly support this general view. Given the relatively shallow topography of the shelf and banks surrounding the Cariaco Basin, it is logical to focus on glacioeustatic sea level change as a prime candidate for driving first-order changes in biogenic productivity and terrigenous sedimentation.

During glacial periods, the Cariaco Basin would have been increasingly isolated from the open Caribbean by lowered sea level. At the maximum lowstand of the LGM (-121 ± 5 m; Fairbanks, 1989),

the principal connection between the basin and the open Caribbean would have been near the western end by Cabo Codera (Fig. 1) at a depth of <30 m, while the Tortuga Bank to the north and topography to the east between Margarita Island and the Araya Peninsula must have been at least partially emergent. Upon first consideration, the clear evidence for oxic LGM conditions in the Cariaco Basin at a time when the basin was so physically isolated is odd. Peterson et al. (1991), citing foraminiferal census data, attributed the oxic conditions of the last glacial to lower surface productivity and reduced oxygen demand resulting from a shift in the locus of upwelling seaward of the then exposed banks. Recently, Lin et al. (1997) and Haug et al. (1998) have extended the productivity argument by focusing on the more direct effect of reduced glacial sill depths on property distributions in the Cariaco Basin. At present, nutrients are advected from depths of 100 m or more to the surface, where they stimulate high productivity along the coast and over the basin. During the LGM lowstand, however, waters spilling over the sill and filling the basin could only have been derived from the upper 30 m or so of the open Caribbean water column, presumably from the very nutrient-depleted waters that characterize the surface. Thus, even if upwelling was physically active within the more restricted confines of the LGM Cariaco Basin, a likely scenario given evidence for stronger and perhaps even more zonal trade winds (e.g., Mix et al., 1986), the upwelled waters should have been nutrient limited to begin with and have sus-

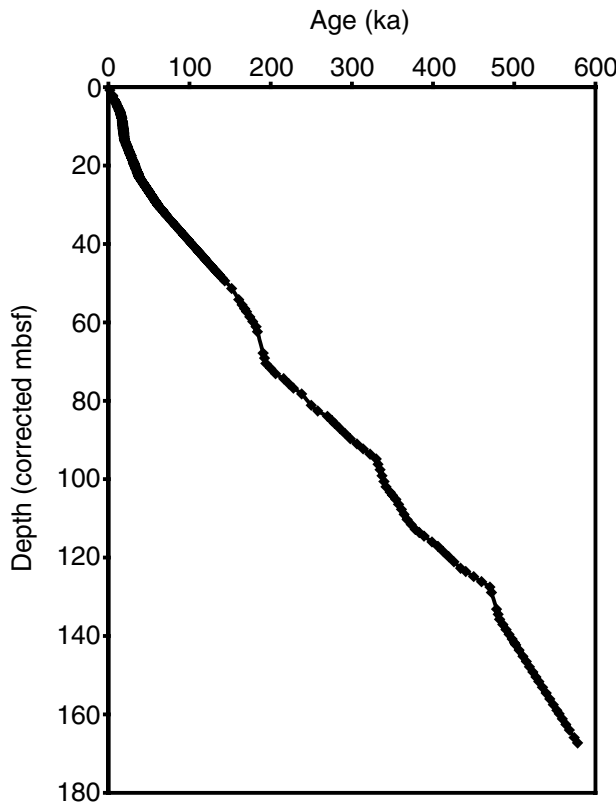


Figure 8. Age-depth function for Hole 1002C derived from the correlation of its $\delta^{18}\text{O}$ record to the SPECMAP stack (Fig. 6). Sedimentation rates at Site 1002 are relatively constant and average ~ 350 m/m.y. over its length.

tained only low biogenic production. Such a situation is likely to have existed during earlier glacials as well, as appears to be reflected in the lower TOC and carbonate contents of the corresponding sediments.

As sea level rose during glacial terminations and the thermocline connection to the open Caribbean became re-established, nutrient supply would be expected to increase and surface production be stimulated. This is clearly illustrated for the most recent deglaciation by the sharp lithologic transition between Subunits IB and IA which occurred at ~ 12.6 ka. According to the reconstruction of Fairbanks (1989), sea level rose little in the early phase of deglaciation between 17.1 and ~ 12.5 ka. This interval was subsequently terminated by a rapid sea-level rise of 24 m in <1000 yr, a rise that correlates in time with peak discharge rates of meltwater (Meltwater Pulse 1-A) into the Gulf of Mexico as recorded by $\delta^{18}\text{O}$ records (e.g., Emiliani et al., 1975; Kennett and Shackleton, 1975; Broecker et al., 1989). The onset of high productivity in the Cariaco Basin, indicated by an abrupt increase in abundance of the upwelling-sensitive *Globigerina bulloides* (Peterson et al., 1991) and by high sediment TOC content and deposition of biogenic opal (Figs. 4, 9), reflects the development of more normal marine conditions as rising sea level enhanced connections with the adjacent Caribbean. Anoxia quickly set in as high productivity and an increased supply of organic detritus overwhelmed the capacity of circulation to ventilate the deep basin. The strong association of well-laminated, diatom-rich sediments and periods of maximum interglacial conditions following abrupt deglaciations (Fig. 4) is consistent with a model of sea level rise causing increased availability of nutrients.

Anoxia occurs whenever the rate of oxygen consumption exceeds the rate of oxygen supply. The presence or absence of anoxic conditions in the marine environment involves complex interactions and balances between biological, chemical, and physical-transport pro-

cesses. Although efforts to date to explain the most recent transition from oxic to anoxic conditions (i.e., 12.6 ka) in the Cariaco Basin have largely focused on oxygen consumption through productivity-related mechanisms, the higher LGM salinities implied by the combination of $\delta^{18}\text{O}$ and alkenone data discussed earlier could also have helped to drive local downwelling that led to greater ventilation of the deep basin. Hólmen and Rooth (1990), based on the analysis of tritium distributions, have implicated the periodic input of warm, salty shelf water as an important ventilation source for the modern Cariaco Basin. Such a process is likely to have been enhanced during the LGM and earlier glacials, given the more restricted nature of the basin and the more arid regional climate (e.g., Van der Hammen, 1974; Schubert, 1988; Clapperton, 1993) that developed in response to a southward shift in the ITCZ and its accompanying rain belt.

In considering the potential role that salinity variations may play in ventilating silled basins, it is of interest to compare the Cariaco Basin setting with that of the much larger Japan Sea (present sill depths of <130 m), which was also relatively isolated during sea-level lowstands of the LGM and earlier glacials. In contrast to the Cariaco Basin, which is anoxic today but was oxygenated during the LGM, the presently well-ventilated Japan Sea experienced anoxic bottom conditions during glacial maxima as indicated by the deposition of dark, organic-rich laminated sediment layers (Oba et al., 1991; Tada et al., 1992). Very light $\delta^{18}\text{O}$ values recorded in planktonic foraminifers during the last glacial led Oba et al. (1991) to suggest that these layers were deposited when the upper water column became stratified by the influx of low-salinity waters, presumably derived from rivers like the Huang Ho whose input was diverted directly into the then more restricted basin.

Despite evidence for increased glacial aridity in northern South America, the relative increase in the terrigenous content of sediments in the Cariaco Basin during sea-level lowstands (Fig. 9) should probably come as no surprise. Today, sources of terrigenous material entering the basin include local rivers that drain directly onto the broad inner shelf region, such as the Manzanares, Tuy, Unare, and Neverí Rivers, as well as the major downstream rivers, the Orinoco and Amazon. During sea-level lowstands, contributions of fine-grained sediments sourced from the more distant Orinoco and Amazon Rivers are expected to have been reduced as the shelf narrowed and their sediments were discharged directly onto the Atlantic continental rise. Observations of Milliman et al. (1982) support this view; carbonate reefs buried beneath upper Holocene muds along the northern Venezuelan coast east of the Cariaco Basin yielded radiocarbon dates between 9.3 and 9.9 ka, leading these authors to speculate that demise of the reefs was caused by some combination of drowning and/or smothering by mud as rising sea level opened connections near Trinidad that permitted Holocene sediment transport from the Orinoco/Amazon systems to begin. Clay mineral studies of Site 1002 sediments indicate that the relative contribution from local rivers to the Cariaco Basin greatly increased during all glacials as lowered sea level reduced the width of the inner shelf from ~ 50 km to only a few kilometers (Clayton et al., in press). Given the proximity of the local river mouths to the edge of the basin at these times, a significant increase in the overall volume of terrigenous sediment input during glacials would probably have been expected.

The long-term ventilation history of the Cariaco Basin can be inferred from the variable distribution at Site 1002 of sediment intervals that are distinctly laminated and intervals that are massive or visibly bioturbated. This is illustrated in Figure 4 where the downhole occurrence of laminated sequences is shown relative to the $\delta^{18}\text{O}$ record of Hole 1002C. Counter to what might be predicted based on earlier discussion of the LGM, the long-term record of anoxia is clearly not a simple one related to glacial-interglacial extremes of sea level, productivity, and/or salinity; much of the time period spanning glacial MIS 3–4 is characterized by intervals of laminated sediments, whereas much of the sediment in interglacial MIS 5, 7, and 9 pre-

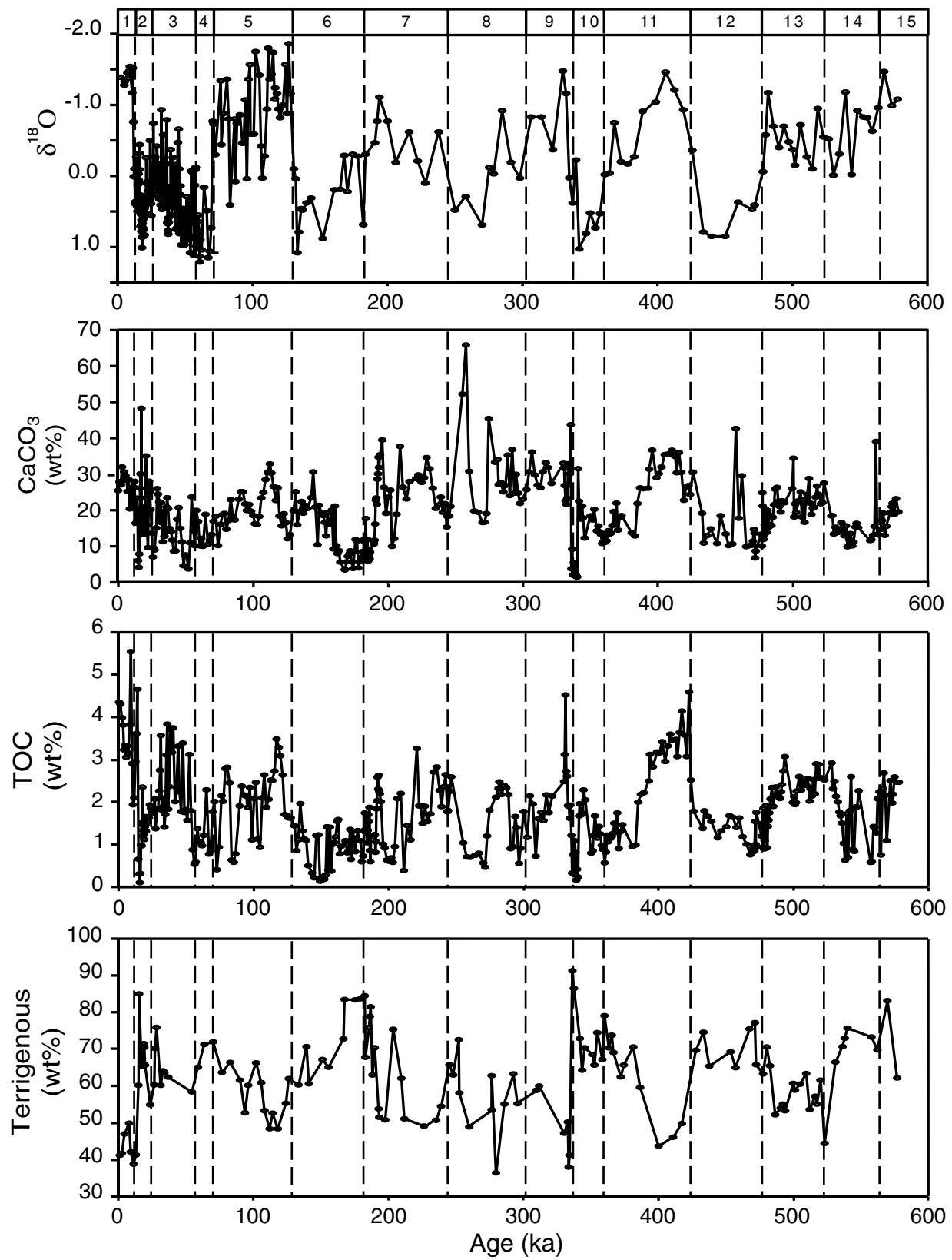


Figure 9. Downhole variations (wt%) in measured calcium carbonate, total organic carbon (TOC), and terrigenous matter in Hole 1002C compared to the $\delta^{18}\text{O}$ stratigraphy for this site. Data are plotted against estimated age using the age model shown in Figure 8. In general, carbonate and TOC contents tend to be high in sediments of interglacial age, whereas terrigenous contents typically increase in glacial sediments.

serves a clear record of bioturbation. Laminated sediments make up much of the Site 1002 sequence deposited before MIS 9, but appear to be less commonly distributed in MIS 6–9. The reasons for this apparently complicated oxygenation history are not yet clear, but are the focus of active investigation. As data from our arsenal of biotic, lithologic, and geochemical proxies continue to grow in shore-based studies, we hope to better understand the relationships and connections between climate, sea level, and depositional history in this small, climatically sensitive basin.

CONCLUSIONS

The 170.1-m-long hemipelagic sediment sequence recovered at ODP Site 1002 in the Cariaco Basin (Venezuela) contains a continuous late Quaternary record that spans the last ~580 k.y. A newly available planktonic foraminiferal $\delta^{18}\text{O}$ stratigraphy, coupled with a revised set of shore-based biostratigraphic datums, clearly indicates that the basal age of Site 1002 is approximately twice as old as initially surmised from the single tentative biostratigraphic identification available from shipboard sampling of core catchers. Sedimentation rates at Site 1002 average in the range of 350 m/m.y., in line with estimates available from shorter piston-core records.

Although $\delta^{18}\text{O}$ variations at Site 1002 can be clearly correlated to the standard open ocean stratigraphy, the amplitude of the glacial-interglacial signal is large, well in excess of 2‰, and there is a significant component of high-frequency variability visible in the record where sampling intervals are close enough to resolve millennial-scale events. Both changes in local sea-surface temperature and salinity offer plausible explanations for the unusual features of the Cariaco Basin $\delta^{18}\text{O}$ record. We consider it likely that the effects of both variables are recorded, with the relative contributions of each varying through time.

Large-scale variations in sediment lithology in the Cariaco Basin can be related to glacial–interglacial climate cycles, most likely as a consequence of glacioeustatic sea-level changes and their effect on basin morphology. During glacial sea-level lowstands, local rivers would have discharged their terrigenous sediment load more directly into the semi-isolated basin, whereas the shallower sill depths would have disrupted the supply of nutrient-rich thermocline waters that support high surface productivity along the Venezuelan coast. These effects can be seen in the changing relative contributions of biogenic carbonate, TOC, and terrigenous matter in the Site 1002 record on glacial–interglacial time scales. Higher frequency variability visible in the records of TOC and carbonate presumably requires a climate/oceanographic mechanism related to circulation and nutrient supply.

The oxygenation history of the Cariaco Basin, as inferred from the presence or absence of preserved sediment laminae, does not appear to be related in a simple way to climate or sea-level cycles of the late Quaternary. Further studies are required to unravel the complicated linkages between climate variability and the processes that control export production, carbon burial, and anoxia in this important tropical setting.

ACKNOWLEDGMENTS

Support for this work came from postcruise funding made available to LCP, RWM, KMY, JWK, and TJB through the U.S. Science Support Program. Stable isotope analyses were also supported by NSF Grant OCE-9709807 to LCP, who acknowledges with thanks the laboratory assistance of K. Blair, H. Ensing, and L. Leist. The contributions of GHH were made possible with funding from the German Research Foundation (DFG) and from NSERC (Canada). Funding to RWM from NSF (EAR-9724282) supported the initial ac-

quisition and use in this study of the ICP-ES facility at Boston University. Postcruise work undertaken by RBP was funded by the NERC (UK). We thank R.C. Thunell and an anonymous reviewer for their constructive and thorough reviews. This is a contribution from the Rosenstiel School of Marine and Atmospheric Science, University of Miami.

REFERENCES

- Athearn, W.D., 1965. Sediment cores from the Cariaco Trench, Venezuela. *Tech. Rep.—Woods Hole Oceanogr. Inst.*, 65–37.
- Broecker, W.S., 1992. The strength of the nordic heat pump. In Bard, E., and Broecker, W.S. (Eds.), *The Last Deglaciation: Absolute and Radiocarbon Chronologies*: Heidelberg (Springer-Verlag), 173–182.
- Broecker, W.S., Kennett, J.P., Flower, B.P., Teller, J.T., Trumbore, S., Bonani, G., and Wölfli, W., 1989. Routing of meltwater from the Laurentide ice sheet during the Younger Dryas cold episode. *Nature*, 341:318–321.
- Clapperton, C.M., 1993. Glacier readvances in the Andes at 12,500–10,000 yr BP: implications for mechanisms of late-glacial climatic change. *J. Quat. Sci.*, 8:197–215.
- Clayton, T., Pearce, R.B., and Peterson, L.C., in press. Indirect climatic control of the clay mineral composition of Quaternary sediments from the Cariaco Basin, northern Venezuela (ODP Site 1002). *Mar. Geol.*
- Curry, W.B., and Oppo, D.W., 1997. Synchronous, high-frequency oscillations in tropical sea surface temperatures and North Atlantic Deep water production during the last glacial cycle. *Paleoceanography*, 12:1–14.
- Dessier, A., and Donguy, J.R., 1994. The sea surface salinity in the tropical Atlantic between 10°S and 30°N: seasonal and interannual variations (1977–1989). *Deep Sea Res.*, 41:81–100.
- Edgar, N.T., Saunders, J.B., et al., 1973. *Init. Repts. DSDP*, 15: Washington (U.S. Government Printing Office).
- Emiliani, C., 1955. Pleistocene temperatures. *J. Geol.*, 63:538–578.
- Emiliani, C., Gartner, S., Lidz, B., Eldridge, K., Elvey, D.K., Huang, T.L., Stipp, J.J., and Swanson, M.F., 1975. Paleoclimatological analysis of late Quaternary cores from the northeastern Gulf of Mexico. *Science*, 189:1083–1088.
- Epstein, S., Buchsbaum, R., Lowenstam, H.A., and Urey, H.C., 1953. Revised carbonate-water isotopic scale. *Geol. Soc. Am. Bull.*, 64:1315–1325.
- Ericson, D.B., Ewing, M., Wollin, G., and Heezen, B.C., 1961. Atlantic deep-sea sediment cores. *Geol. Soc. Am. Bull.*, 72:193–286.
- Ericson, D.B., and Wollin, G., 1968. Pleistocene climates and chronology in deep-sea sediments. *Science*, 162:1227–1234.
- Fairbanks, R.G., 1989. A 17,000-year glacio-eustatic sea level record: influence of glacial melting rates on the Younger Dryas event and deep-ocean circulation. *Nature*, 342:637–642.
- Greenland Ice-core Project (GRIP) Members, 1993. Climate instability during the last interglacial period recorded in the GRIP ice core. *Nature*, 364:203–207.
- Halicz, E., and Reiss, Z., 1981. Paleoecological relations of foraminifera in a desert-enclosed sea: the Gulf of Aqaba (Elat), Red Sea. *Mar. Ecol.*, 2:15–34.
- Hastenrath, S., 1978. On modes of tropical circulation and climate anomalies. *J. Atmos. Sci.*, 35:2222–2231.
- , 1990. Diagnostics and prediction of anomalous river discharge in northern South America. *J. Climate*, 3:1080–1096.
- Haug, G.H., Pedersen, T.F., Sigman, D.M., Calvert, S.E., Nielsen, B., and Peterson, L.C., 1998. Glacial/interglacial variations in production and nitrogen fixation in the Cariaco Basin during the last 580 kyr. *Paleoceanography*, 13:427–432.
- Hay, W.W., and Beaudry, F.M., 1973. Calcareous nannofossils—Leg 15, Deep Sea Drilling Project. In Edgar, N.T., Saunders, J.B., et al., *Init. Repts. DSDP*, 15: Washington (U.S. Govt. Printing Office), 625–683.
- Heezen, B.C., MacGregor, I.D., et al., 1973. *Init. Repts. DSDP*, 20: Washington (U.S. Govt. Printing Office).
- Heezen, B.C., Menzies, R.J., Broecker, W.S., and Ewing, M., 1958. Date of stagnation of the Cariaco Trench, southeast Caribbean. *Geol. Soc. Am. Bull.*, 69:1579. (Abstract)
- Heezen, B.C., Menzies, R.J., Broecker, W.S., and Ewing, W.M., 1959. Stagnation of the Cariaco Trench. In Sears, M. (Ed.), *International Oceanography Congress*, Am. Assoc. for Adv. Sci., 99–102.

- Herrera, L.E., and Febres-Ortega, G., 1975. Procesos de surgencia y de renovación de aguas en la Fosa de Cariaco, Mar Caribe. *Bol. Inst. Oceanogr. Univ. Oriente*, 14:31–44.
- Hólmen, K.J., and Rooth, C.G.H., 1990. Ventilation of the Cariaco Trench, a case of multiple source competition? *Deep-Sea Res.*, 37:203–225.
- Hughen, K.A., Overpeck, J.T., Lehman, S.J., Kashgarian, M., Southon, J., Peterson, L.C., Alley, R., and Sigman, D.M., 1998. Deglacial changes in ocean circulation from an extended radiocarbon calibration. *Nature*, 391:65–68.
- Hughen, K., Overpeck, J.T., Peterson, L.C., and Anderson, R.F., 1996. The nature of varved sedimentation in the Cariaco Basin, Venezuela, and its palaeoclimatic significance. In Kemp, A.E.S. (Ed.), *Palaeoclimatology and Palaeoceanography from Laminated Sediments*. Geol. Soc. Spec. Publ. London, 116:171–183.
- Hughen, K., Overpeck, J.T., Peterson, L.C., and Trumbore, S.E., 1996. Rapid climate changes in the tropical Atlantic during the last deglaciation. *Nature*, 380:51–54.
- Imbrie, J., Hays, J.D., Martinson, D.G., McIntyre, A., Mix, A.C., Morley, J.J., Pisias, N.G., Prell, W.L., and Shackleton, N.J., 1984. The orbital theory of Pleistocene climate: support from a revised chronology of the marine $\delta^{18}\text{O}$ record. In Berger, A., Imbrie, J., Hays, J., Kukla, G., and Saltzman, B. (Eds.), *Milankovitch and Climate* (Pt. 1), NATO ASI Ser. C, Math Phys. Sci., 126:269–305.
- Kennett, J.P., and Shackleton, N.J., 1975. Laurentide Ice Sheet meltwater recorded in Gulf of Mexico deep-sea cores. *Science*, 188:147–150.
- Lidz, L., Charm, W.B., Ball, M.M., and Valdes, S., 1969. Marine basins off the coast of Venezuela. *Bull. Mar. Sci.*, 19:1–17.
- Lin, H.-L., Peterson, L.C., Overpeck, J.T., Trumbore, S.E., and Murray, D.W., 1997. Late Quaternary climate change from $\delta^{18}\text{O}$ records of multiple species of planktonic foraminifera: high-resolution records from the anoxic Cariaco Basin (Venezuela). *Paleoceanography*, 12:415–427.
- Locke, S., and Thunell, R.C., 1988. Paleoceanographic record of the last glacial/interglacial cycle in the Red Sea and Gulf of Aden. *Palaeogeogr., Palaeoclimatol., Palaeoecol.*, 64:163–187.
- McIver, R.D., 1973. Cyclical geochemical properties of organic matter in Cariaco Basin cores, Leg 15, Site 147. In Heezen, B.C., and MacGregor, I.D., et al., *Init. Repts. DSDP*, 20: Washington (U.S. Govt. Printing Office), 935–936.
- Milliman, J.D., Butenko, J., Barbot, J.P., and Hedberg, J., 1982. Depositional patterns of modern Orinoco/Amazon muds on the northern Venezuelan shelf. *J. Mar. Res.*, 7:643–657.
- Mix, A.C., Ruddiman, W.F., and McIntyre, A., 1986. The late Quaternary paleoceanography of the tropical Atlantic. 1: Spatial variability of annual mean sea-surface temperatures, 0–20,000 years B.P. *Paleoceanography*, 1:43–66.
- Muller-Karger, F.E., and Aparicio-Castro, R., 1994. Mesoscale processes affecting phytoplankton abundances in the southern Caribbean Sea. *Cont. Shelf Res.*, 14:199–221.
- Murray, R.W., and Leinen, M., 1993. Chemical transport to the seafloor of the equatorial Pacific Ocean across a latitudinal transect at 135°W: tracking sedimentary major, trace, and rare earth element fluxes at the Equator and the Intertropical Convergence Zone. *Geochim. Cosmochim. Acta*, 57:4141–4163.
- , 1996. Scavenged excess aluminum and its relationship to bulk titanium in biogenic sediment from the central Pacific Ocean. *Geochim. Cosmochim. Acta*, 60:3869–3878.
- Oba, T., Kato, M., Kitazato, H., Koizumi, I., Omura, A., Sakai, T., and Takayama, T., 1991. Paleoenvironmental changes in the Japan Sea during the last 85,000 years. *Paleoceanography*, 6:499–518.
- Okada, H., and Bukry, D., 1980. Supplementary modification and introduction of code numbers to the low-latitude coccolith biostratigraphic zonation (Bukry, 1973; 1975). *Mar. Micropaleontol.*, 5:321–325.
- Overpeck, J.T., Peterson, L.C., Kipp, N., Imbrie, J., and Rind, D., 1989. Climate change in the circum-North Atlantic region during the last deglaciation. *Nature*, 338:553–557.
- Peterson, L.C., Overpeck, J.T., Kipp, N.G., and Imbrie, J., 1991. A high-resolution late Quaternary upwelling record from the anoxic Cariaco Basin, Venezuela. *Paleoceanography*, 6:99–119.
- Piper, D.J.W., and Flood, R.D., 1997. Preface: depth below seafloor conventions. In Flood, R.D., Piper, D.J.W., Klaus, A., and Peterson, L.C. (Eds.), *Proc. ODP, Sci. Results*, 155: College Station, TX (Ocean Drilling Program), 3–4.
- Prell, W.L., and Damuth, J.E., 1978. The climate related diachronous disappearance of *Pulleniatina obliquiloculata* in Late Quaternary sediments of the Atlantic and Caribbean. *Mar. Micropaleontol.*, 3:267–277.
- Rau, G., 1994. Variations in sedimentary organic $\delta^{13}\text{C}$ as a proxy for past changes in ocean and atmospheric CO_2 changes. *NATO ASI Ser. I, Glob. Environ. Change*, 17:307–321.
- Richards, F.A., 1975. The Cariaco Basin (Trench). *Annu. Rev. Oceanogr. Mar. Biol.*, 13:11–67.
- Rögl, F., and Bolli, H.M., 1973. Holocene to Pleistocene planktonic foraminifera of Leg 15, Site 147 (Cariaco Basin [Trench], Caribbean Sea) and their climatic interpretation. In Edgar, N.T., Saunders, J.B., et al., *Init. Repts. DSDP*, 15: Washington (U.S. Govt. Printing Office), 553–615.
- Schubert, C., 1982. Origin of Cariaco Basin, southern Caribbean Sea. *Mar. Geol.*, 47:345–360.
- , 1988. Climatic changes during the last glacial maximum in northern South America and the Caribbean: a review. *Interciencia*, 13:128–137.
- Shipboard Scientific Party, 1997a. Explanatory notes. In Sigurdsson, H., Leckie, R.M., Acton, G.D., et al., *Proc. ODP, Init. Repts.*, 165: College Station, TX (Ocean Drilling Program), 15–46.
- , 1997b. Site 1002. In Sigurdsson, H., Leckie, R.M., Acton, G.D., et al., *Proc. ODP, Init. Repts.*, 165: College Station, TX (Ocean Drilling Program), 359–373.
- Sigurdsson, H., Leckie, R.M., Acton, G.D., et al., 1997. *Proc. ODP, Init. Repts.*, 165: College Station, TX (Ocean Drilling Program).
- Tada, R., Koizumi, I., Cramp, A., and Rahman, A., 1992. Correlation of dark and light layers, and the origin of their cyclicity in the Quaternary sediments from the Japan Sea. In Pisciotto, K.A., Ingle, J.C., Jr., von Breymann, M.T., Barron, J., et al., *Proc. ODP, Sci. Results*, 127/128 (Pt. 1): College Station, TX (Ocean Drilling Program), 577–601.
- Taylor, S.R., and McLennan, S.M., 1985. *The Continental Crust: Its Composition and Evolution*. Oxford (Blackwell Scientific).
- Thierstein, H.R., Geitzenauer, K., Molino, B., and Shackleton, N.J., 1977. Global synchronicity of late Quaternary coccolith datum levels: validation by oxygen isotopes. *Geology*, 5:400–404.
- Van der Hammen, T., 1974. The Pleistocene changes of vegetation and climate in tropical South America. *J. Biogeogr.*, 1:3–26.
- Wakeham, S.G., and Ertel, J.R., 1988. Diagenesis of organic matter in suspended particles in sediments in the Cariaco Trench. *Org. Geochem.*, 13:815–822.
- Wüst, G., 1964. *Stratification and Circulation in the Antillean-Caribbean Basins*. New York (Columbia Univ. Press).

Date of initial receipt: 23 June 1998**Date of acceptance: 21 May 1999****Ms 165SR-017**